

Computationally efficient worst-case analysis of flow-controlled networks with Network Calculus

Raffaele Zippo, Giovanni Stea

Abstract

Networks with hop-by-hop flow control occur in several contexts, from data centers to systems architectures (e.g., wormhole-routing networks on chip). A worst-case end-to-end delay in such networks can be computed using Network Calculus (NC), an algebraic theory where traffic and service guarantees are represented as curves in a Cartesian plane. NC uses transformation operations, e.g., the min-plus convolution, to model how the traffic profile changes with the traversal of network nodes. NC allows one to model flow-controlled systems, hence one can compute the end-to-end *service curve* describing the minimum service guaranteed to a flow traversing a tandem of flow-controlled nodes. However, while the algebraic expression of such an end-to-end service curve is quite compact, its computation is often untractable from an algorithmic standpoint: data structures tend to explode, making operations unfeasibly complex, even with as few as three hops.

In this paper, we propose computational and algebraic techniques to mitigate the above problem. We show that existing techniques (such as reduction to *compact domains*) cannot be used in this case, and propose an arsenal of solutions, which include methods to mitigate the data representation space explosion as well as computationally efficient algorithms for the min-plus convolution operation. We show that our solutions allow a significant speedup, enable analysis of previously unfeasible case studies, and – since they do not rely on any approximation – still provide exact results.

Index Terms

Network Calculus, Worst-case Delay Bounds, Computer Networks.

I. INTRODUCTION

The last few years have witnessed a surge in real-time networked applications, such as factory automation or collaborative robotics, within the Industry 4.0 paradigm, or self-driving / teleoperated cars. This has sparked a renewed industrial interest for methods that allow one to compute *performance bounds*, especially worst-case ones, since the above applications are clearly safety critical. Several systems supporting these applications communicate through networks with hop-by-hop window flow control. This occurs whenever a receiver has limited buffer space and wants to prevent the sender from overflowing it – because the loss of data is undesirable or too costly. This mechanism is used, for instance, in data center networks [1]–[3], or wormhole-routing networks on chip [4], [5]. Multi-hop networks with flow control have often been analyzed via classical queueing theory (see, e.g., [6]), that allows one to find probabilistic performance metrics using stochastic models of traffic and service. A worst-case analysis of such networks can be done via Network Calculus (NC). The latter is a theory for deterministic network evaluation, which dates back to the early 1990s, and it is mainly due to the work of Cruz [7], [8], Le Boudec and Thiran [9], and Chang [10]. Originally devised for the Internet, where it was used to engineer models of service [11]–[15], it has found applications in several other contexts, from sensor networks [16] to avionic networks [17], [18], industrial networks [19]–[21] automotive systems [22] and systems architecture [23], [24]. Its main strength is that it allows one to compute worst-case delay bounds in systems with multi-hop traversal. It characterizes constraints on traffic arrivals (due to traffic shaping) and on minimum received service (due to scheduling) as *curves*, i.e., functions of time, and uses min-plus algebra to combine the above in order to compute bounds on the traffic at any point in a network traversal. More in detail, a network node is characterized by its *service curve*, a characteristic function that yields the worst-case response to an infinite burst (similarly to the transfer function in systems theory). When a flow traverses two nodes in tandem, its worst-case end-to-end service can be found by combining the service curves of the two nodes via their *min-plus convolution*. This operation yields a network-wide service curve, hence multi-node traversal can always be collapsed to single-node traversal via repeated convolutions. Most network nodes have simple service curves, called *rate-latency*, that can be represented by two segments: an initial horizontal segment – modeling the node’s latency – followed by an infinite line whose slope is the node’s rate. The convolution of two rate-latency curves is a rate-latency curve itself.

Window flow control can be modeled in NC. The algebraic operator that is required to do this is called *sub-additive closure* (SAC), which – as the name suggests – yields sub-additive curves. A flow-controlled node can thus be represented via an *equivalent* service curve, obtained via a SAC operation. Analysis of networks with hop-by-hop flow-control is made difficult by computational aspects. An equivalent service curve obtained via a SAC is unavoidably a staircase-based ultimately pseudo-periodic (UPP) function [25], [26], even when the node has a service curve as simple as a rate-latency one. UPP functions have

R. Zippo is with Dipartimento di Ingegneria dell’Informazione, Università di Firenze, Via di S. Marta 3, 50139 Firenze, Italy. e-mail: raffaele.zippo@unifi.it

R. Zippo and G. Stea are with Dipartimento di Ingegneria dell’Informazione, Università di Pisa, Largo Lucio Lazzarino 1, 56122 Pisa, Italy. e-mail: giovanni.stea@unipi.it, raffaele.zippo@phd.unipi.it

an initial transient and a periodic part. Computing the worst-case delay of a flow traversing a tandem of flow-controlled hops requires one to compute an *end-to-end equivalent service curve* for the tandem first. However, this requires one to compute *nested* SACs, starting from per-node service curves. The algorithm to compute the SAC of an UPP curve is very complex, to the point that this analysis may be computationally unfeasible already with few hops (e.g., three). The SAC algorithm, in fact, requires performing a very large number of elementary convolutions. Work [27] introduces a different method, which dispenses with nested SACs. That method computes *per-node* equivalent service curves first, using SAC, and then computes the end-to-end equivalent service curve by *convolution* of per-node equivalent service curves. This second method yields an end-to-end equivalent service curve that lower bounds the one found with the former method. It is also less costly, since convolution of UPP curves is polynomial. However, chained convolutions of UPP curves may still be unfeasibly costly, due to a well-known phenomenon called *state explosion* ([28], [29]). It is observed therein that convolutions of UPP functions tend to explode, because the period of the result is tied to the least common multiple (*lcm*) of the periods of the operands. Thus, computing the end-to-end service curve of a tandem of N nodes traversed by a flow by chaining $N - 1$ convolutions – although *algebraically* simple – is often *computationally* intractable.

In [29], authors propose a method to mitigate this problem by observing that one may limit convolutions to a *compact* (i.e., finite) domain, without sacrificing accuracy. That finite domain is computed (at negligible cost) based on upper/lower approximations of UPP service curves and/or arrival curves. Using finite domains allows one to avoid the state explosion due to the *lcm* and the associated time complexity, making analysis faster – often by orders of magnitude. However, this method cannot be applied to our problem, since it relies on service curves being *super-additive*. The equivalent service curves that form the operands of the chained convolutions in our problem are instead *sub-additive* (having been computed via a SAC operation).

In this paper, we present computational and algebraic techniques to enable the analysis of flow-controlled networks on a larger scale, by reducing the number and time cost of the involved convolutions, often by orders of magnitude. We achieve this by performing two computationally simple tasks: first, minimizing the number of segments with which a UPP service curve is represented. This is particularly important, since – on one hand – the complexity of algorithms for basic min-plus operations (including convolution) depends on the number of segments of their operands, often in a superlinear way. On the other hand, the *number* of convolutions to be performed in a SAC depends on the number of segments of the operand. We show that *representation minimization* may reduce the number of segments by orders of magnitude. This makes operations generally faster – especially when several convolutions are chained together, and is of paramount importance to enable efficient SAC computation. Second, we prove algebraic properties of sub-additive functions that can be leveraged to drastically reduce the number of computations involved in the convolution. We prove that convolution of sub-additive UPP functions is in fact quite simple, unless the two operands intersect infinitely many times, and we prove a significantly faster algorithm for that case as well. We assess the gain in efficiency by measuring the achieved speedup of our findings on a desktop PC. As we show, the improvements are substantial, ranging from two-digit percentages to several orders of magnitude in most cases. Moreover, the speedups warranted by representation minimization and algebraic properties are cumulative. This not only makes computations more efficient: rather, it allows one to compute end-to-end service curves in cases where this was considered to be beyond the borders of tractability using the current NC methods and off-the-shelf hardware. Moreover, it allows one to compare the two methods discussed above, hence to benchmark the lower-bound approximation explained in [27] by efficiency and accuracy. Our findings in that respect are that the approximate method seems to be as accurate as the exact one, while considerably more efficient. Last, but not least, we remark that our techniques are *exact*, i.e., they do not entail any loss of accuracy in the end result. To the best of our knowledge, our results are novel and are not used in existing NC tools.

The rest of the paper is organized as follows: Section II introduces NC notation and basic results. We introduce the problem formally in Section III, and explain our techniques in Section IV. We report numerical evaluations in Section V. Section VI discusses the related works. Finally, Section VII concludes the paper and highlights directions for future work.

II. NETWORK CALCULUS BASICS

We report here a necessarily concise introduction to NC, borrowing the notation used in [9], to which we refer the interested reader for more details.

A NC flow is represented as a wide-sense increasing and left-continuous cumulative function $R : \mathbb{R}_+ \rightarrow \mathbb{R}_+$. Function $R(t)$ represents the number of bits of the flow observed in $[0, t]$. In particular, $R(0) = 0$.

Flows can be constrained by *arrival curves*. A wide-sense increasing function α is an *arrival curve* for a flow A if:

$$\forall s \leq t, \quad A(t) - A(s) \leq \alpha(t - s).$$

For instance, a *leaky-bucket shaper*, with a *rate* ρ and a *burst size* σ , enforces the concave affine arrival curve $\gamma_{\sigma, \rho}(t) = \sigma + \rho t$. This means, among other things, that the long-term arrival rate of the flow cannot exceed ρ .

Let A and D be the functions that describe the same data flow at the input and output of a lossless network element (or *node*), respectively. If that node does not create data internally (which is often the case), causality requires that $A \geq D$. We say that the node behavior can be modeled via a *service curve* β if:

$$\forall t \geq 0, \quad D(t) \geq \inf_{0 \leq s \leq t} A(s) + \beta(t - s). \quad (1)$$

In that case, the flow is guaranteed the (minimum) service curve β . The infimum on the right side of Eq. (1), as a function of t , is called the (*min-plus*) *convolution* of $A(t)$ and $\beta(t)$, and is denoted by $(A \otimes \beta)(t)$. The dependency from t is omitted whenever it is clear from the context. The alert reader can check that convolution is commutative and associative. Computing the above convolution entails sliding β along A and taking the *lower envelope* of the result (i.e., the infimum for each time instant).

Several network elements, such as delay elements, schedulers or links, can be modeled through service curves. A very frequent case is the one of *rate-latency* service curves, defined as:

$$\beta_{\theta,R}(t) = R(t - \theta)_+.$$

for some $\theta > 0$ (the latency) and $R > 0$ (the rate). Notation $(.)_+$ denotes $\max(., 0)$. For instance, a constant-rate server (e.g., a wired link) can be modeled as a rate-latency curve with a null latency.

A point of strength of NC is that service curves are *composable*: the end-to-end service curve of a tandem of nodes traversed by the same flow can be computed as the convolution of the service curves of each node.

For a flow that traverses a service curve (be it the one of a single node, or the end-to-end service curve of a tandem computed as discussed above), a tight *upper bound* on the delay can be computed by combining its arrival curve α and the service curve β itself, as follows:

$$h(\alpha, \beta) = \sup_{t \geq 0} [\inf \{d \geq 0 \mid \alpha(t - d) \leq \beta(t)\}]. \quad (2)$$

The quantity $h(\alpha, \beta)$ is in fact the maximum horizontal distance between α and β . Therefore, computing the end-to-end service curve of a flow in a tandem traversal is the crucial step towards obtaining its worst-case delay bound.

In NC, the *sub-additive closure (SAC)* of a wide-sense increasing function f is defined as:

$$\overline{f(t)} = \inf_{n \geq 0} [f^{(n)}(t)] \quad (3)$$

where $f^{(n)}$ denotes the convolution of f with itself n times, and $f^{(0)}$ is an infinite step at $t = 0^+$. Note that \overline{f} is sub-additive, as the name suggests. The formal definition of sub-additivity is the following:

Definition 1 (Sub-additive function). f is sub-additive if and only if $f(u) + f(s) \geq f(u + s) \forall u, s$.

Moreover, if f is sub-additive, it is $\overline{f} = f$. Otherwise, it is $\overline{f} \leq f$. Convolution does preserve sub-additivity, as per the following property:

Property 1 (Convolution of sub-additive functions). If f and g are sub-additive functions, so is $f \otimes g$ [9, Theorem 3.1.9].

and the SAC of a minimum is the convolution of the SACs of the operands, i.e.:

Property 2 (SAC of a minimum). $\overline{f \wedge g} = \overline{f} \otimes \overline{g}$ [9, Theorem 3.1.11]

A. Computational representation of NC functions and algorithms

NC computations can be implemented in software. In order to do so, one needs to provide computational representations of NC functions (e.g., a cumulative function of a flow or a service curve) and well-formed algorithms for its operations, e.g., minimum and convolution. We therefore describe a general data structure that represents NC functions, and the algorithms to compute the main NC operations used in this paper. We adopt the widely accepted approach described in [25], [26].

An NC function can be represented by an ultimately pseudo-periodic piecewise affine $\mathbb{Q}_+ \rightarrow \mathbb{Q}$ function. In [25], this class of functions is shown to be stable w.r.t. all min-plus operations, while functions $\mathbb{R}_+ \rightarrow \mathbb{R}$ are not¹. For such a function, it is enough to store a representation of the initial transient part and of one period, which is a finite amount of information. With reference to Figure 1, let T denote the length of the initial transient, and let d and c denote the length and height of a period. Pseudo-periodicity means that: $\forall t \geq T, f(t + d) = f(t) + c$.

Accordingly, we call a *representation* R_f of a function f the tuple (S, T, d, c) , where T, d, c are the values described above, and S is a sequence of points and open segments describing f in $[0, T + d[$. We use both points and open segments in order to easily model discontinuities. We will use the umbrella term *elements* to encompass both, when convenient. For example, for a rate-latency curve $\beta_{\theta,R}$ we have $T = \theta$, d and c can be arbitrary positive numbers such that $c/d = R$, and S is a list of four elements: point $(0, 0)$, segment $(0, 0) \rightarrow (\theta, 0)$, point $(\theta, 0)$, segment $(\theta, 0) \rightarrow (\theta + d, c)$.

Note that, given R_f , one can compute $f(t)$ for any $t \geq 0$. Furthermore, being finite, R_f can be used as the data structure to represent f in code. We also define the following quantities, that will be used throughout the paper: let ρ_f be the pseudo-periodic slope of f , i.e., $\rho_f = \frac{c_f}{d_f}$. Moreover, call S_f^D the sequence of elements, adequately computed from R_f , describing f over interval D . Accordingly, let us define S_f^T and S_f^P as the transient (i.e., in $[0, T[$) and pseudo-periodic (i.e., in $[T, T + d[$) parts of S . Given a sequence S , we define its *cardinality* $N(S)$ as the number of elements it contains.

¹An alternative class of functions with such stability is $\mathbb{N} \rightarrow \mathbb{R}$, however this is only feasible for models where time is discrete.

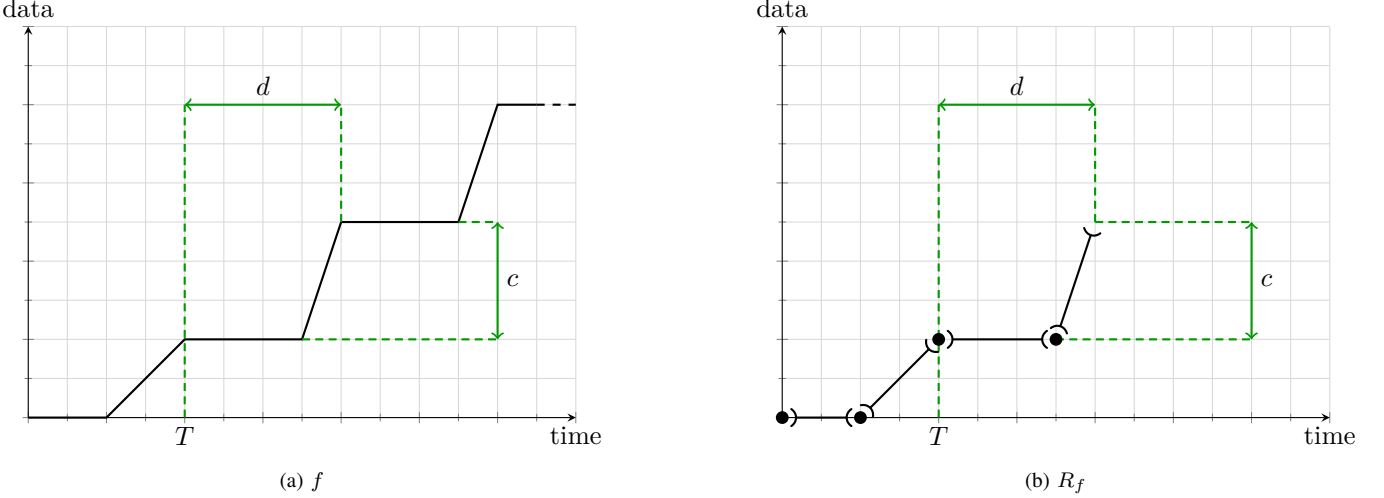


Fig. 1. Example of ultimately pseudo-periodic piecewise affine function f and its representation R_f

As outlined in the Introduction, the aim of this paper is to present new techniques to reduce the computation times of NC computations. We therefore need to introduce the basic algorithms for NC operations, i.e., equivalence, minimum, convolution and SAC. A complete description of the algorithms for the above operations would be cumbersome, and would distract the reader from the main focus of this work. For this reason, we sketch here the basic results required for the understanding of the rest of the paper, and refer the interested reader to the Appendix for more details.

Given two representations R_f and R_g we can establish if $f = g$ through a linear comparison of the representations in $D = [0, \max(T_f + 2d_f, T_g + 2d_g)[$. The alert reader can check that if $f(t) = g(t) \forall t \in D$, then $f(t) = g(t) \forall t \geq 0$. The complexity of such comparison is then $O(N(S_f^D) + N(S_g^D))$.

Binary NC operations (such as minimum and convolution) take as input the representations of operands and produce as an output the representation of the result. Given two functions f and g and a *generic* operator $*$, in order to compute $f * g$ we need an algorithm that computes R_{f*g} from R_f, R_g , i.e., $(R_f, R_g) \rightarrow R_{f*g}$. This is generally done via the following steps:

- 1) Compute valid parameters T_{f*g}, d_{f*g} and c_{f*g} ;
- 2) Compute the domains D_f and D_g necessary to compute $S_f^{D_f}$ and $S_g^{D_g}$;
- 3) Compute $(S_f^{D_f}, S_g^{D_g}) \rightarrow S_{f*g}$, i.e., provide an algorithm that computes the resulting sequence from the sequences of the operands (which we call *by-sequence* implementation of operator $*$);
- 4) Return $R_{f*g} = (S_{f*g}, T_{f*g}, d_{f*g}, c_{f*g})$.

For the *minimum* operator, i.e., $m = f \wedge g$, the by-sequence algorithm is a linear comparison of sequences $S_f^{D_f}, S_g^{D_g}$, hence its complexity is $O(N(S_f^{D_f}) + N(S_g^{D_g}))$. However, it may well be that $N(S_f^{D_f}) \gg N(S_f)$ and/or $N(S_g^{D_g}) \gg N(S_g)$, depending on numerical properties of f and g . For instance, when f and g have different slopes ρ_f, ρ_g , and intersect at $\bar{t} \gg T_f + d_f, T_g + d_g$. This means that the computations involved in an operation may vary considerably based on numerical properties of the operands. This issue will be recalled time and again throughout this paper.

For what concerns the *convolution* operation, we observe that in the general case it is not possible to compute the parameters and domains of step 1 and 2 *a priori*. To circumvent this, [26] proposes to decompose each operand f into its transient and periodic parts, f_t and f_p , each assuming value $+\infty$ outside their domain, so that $f = f_t \wedge f_p$. Therefore, convolution $f \otimes g$ can be decomposed as:

$$f \otimes g = (f_t \wedge f_p) \otimes (g_t \wedge g_p) = f_t \otimes g_t \wedge f_t \otimes g_p \wedge f_p \otimes g_t \wedge f_p \otimes g_p \quad (4)$$

Equation (4) highlights three types of partial convolutions: transient part with transient part; transient part with periodic part; periodic part with periodic part. For these partial convolutions, parameters and domains can instead be computed. After all the partial convolutions in Equation (4) have been computed, the end result can be obtained by taking the minimum of all partial results. A notable exception, which will be useful for this work, is when $\rho_f = \rho_g$. In this case, in fact, domains and parameters can be computed *a priori* as follows:

$$T' = T_f + T_g + d'; \quad d' = \text{lcm}(d_f, d_g); \quad c' = \rho \cdot d'; \quad D_f = [0, T_f + 2 \cdot d'[; \quad D_g = [0, T_g + 2 \cdot d'[$$

The by-sequence algorithm consists in computing the convolutions of all the elements in the two extended sequences $S_f^{D_f}, S_g^{D_g}$, i.e., all $e_f \otimes e_g$ where $e_f \in S_f^{D_f}, e_g \in S_g^{D_g}$, and taking the lower envelope of the result. The complexity of this operation is $O(N(S_f^{D_f}) \cdot N(S_g^{D_g}) \cdot \log(N(S_f^{D_f}) \cdot N(S_g^{D_g})))$. This complexity is heavily affected by the cardinalities of the

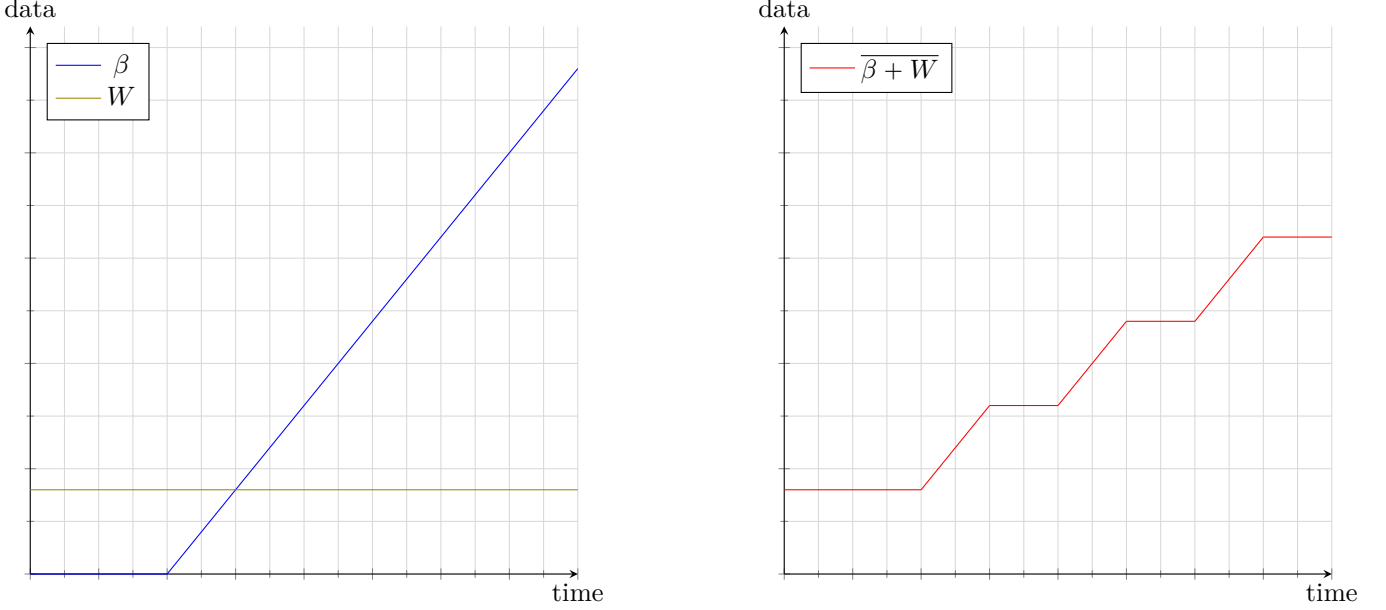


Fig. 2. A SAC can be easily computed if the service curve involved is rate-latency.

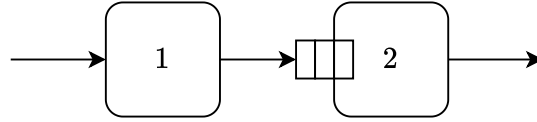


Fig. 3. Network with static window flow-control

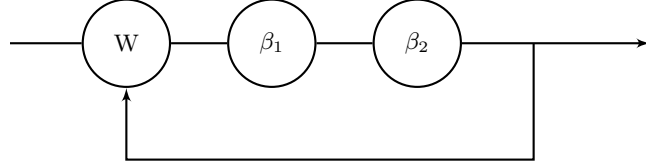


Fig. 4. NC model for network with static window flow-control.

extended sequences, which in turn are tied to $\text{lcm}(d_f, d_g)$. Once again, it is possible that $N(S_f^{D_f}) \gg N(S_f)$, $N(S_g^{D_g}) \gg N(S_g)$, for instance when d_f, d_g are coprime.

The algorithm for computing SAC is based on Property 2. Considering the elements e_i of the sequence of the representation of f , we have $f = e_1 \wedge \dots \wedge e_n \Rightarrow \bar{f} = \bar{e}_1 \otimes \dots \otimes \bar{e}_n$. Thus f is decomposed in points, open segments, pseudo-periodic points and pseudo-periodic open segments, for which algorithms that compute their respective SACs are known [26]. Computing SAC through this algorithm is \mathcal{NP} -hard: the complexity grows exponentially with the number of elements in the representation. We remark that the above algorithm makes extensive use of the convolution operation.

An exception is when β is a rate-latency curve. In this case, given a *constant function*, i.e. a function f such that $f(0) = 0$, $f(t) = W \forall t > 0$, SAC $\overline{\beta + W}$ can be computed in closed form [9]. From now on, we will sometimes refer to positive constants W (typically, buffer dimensions) to denote constant functions. As shown in Figure 2, the resulting function is not a rate-latency, but an UPP function.

B. Flow-controlled networks

NC can be used to model network elements having flow control [9, Chapter 4]. Consider the network in Figure 3, in which a flow traverses nodes 1 and 2, which have static flow-control due to the limited buffer in 2. Node 1 will thus serve traffic, with service curve β_1 , only if there is already buffer space available in 2; in turn, the available part of this buffer space, whose size is W , depends on the ability of 2 to serve traffic with its own service curve β_2 . We also assume that 1 is instantaneously aware of the current state of the buffer of 2. Thus we can model the network as in Figure 4.

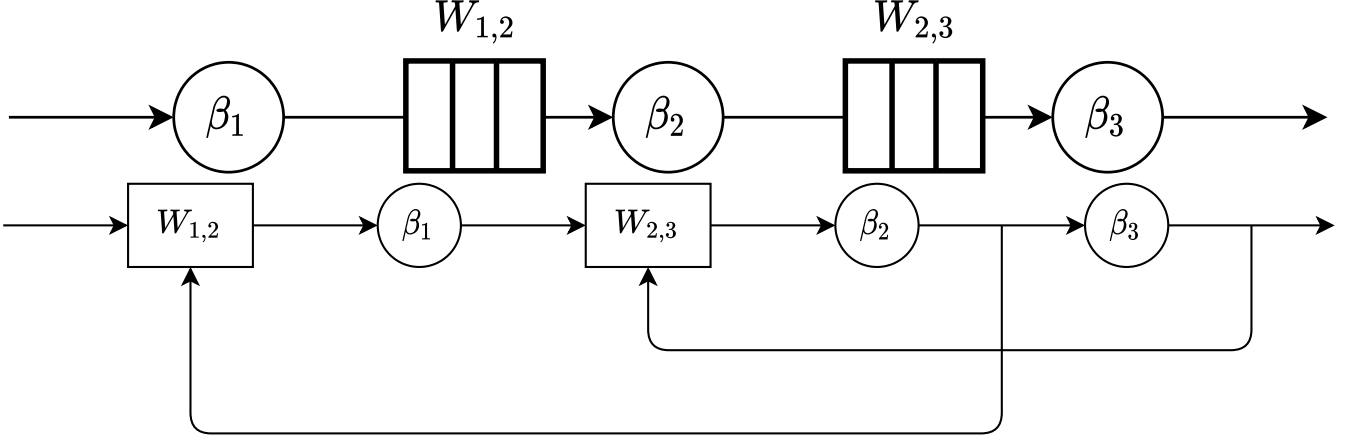


Fig. 5. A tandem of three flow-controlled nodes and its NC model

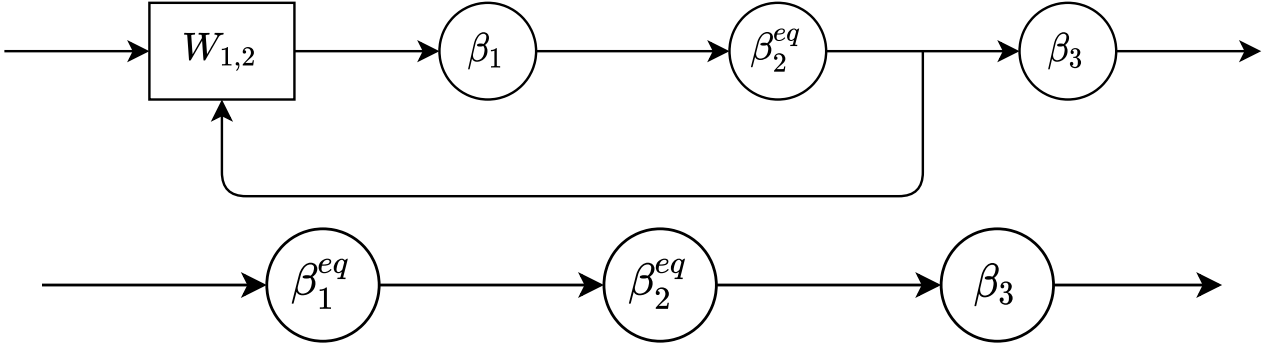


Fig. 6. Transformation of the NC model to an equivalent tandem

In order to compute an end-to-end service curve for a flow traversing the above system, we must first get rid of the feedback arc in the NC model, transforming it into a tandem. This is done by computing first the *equivalent service curve* of node 1, β_1^{eq} . The latter takes into account the reduction in the service brought on by the presence of the subsequent flow control. It is:

$$\begin{aligned}\beta_1^{eq} &= \beta_1 \otimes \beta_{fc} \\ \beta_{fc} &= \overline{\beta_1 \otimes \beta_2 + W}\end{aligned}$$

Then the system offers to the flow an end-to-end service curve β^{eq} equal to:

$$\begin{aligned}\beta^{eq} &= \beta_1^{eq} \otimes \beta_2 \\ &= \beta_1 \otimes \beta_2 \otimes \beta_{fc}\end{aligned}\tag{5}$$

The extension of the above method to longer tandems is straightforward: consider for instance the tandem in Section II-B. Nodes 2 and 3 have limited buffers, of size $W_{1,2}$ and $W_{2,3}$. The resulting NC model is shown in the figure. To find the end-to-end service curve of the system, β^{eq} , we iterate the above methodology – starting from the rightmost node – and compute the following:

$$\begin{aligned}\beta_2^{eq} &= \beta_2 \otimes \overline{\beta_2 \otimes \beta_3 + W_{2,3}} \\ \beta_1^{eq} &= \beta_1 \otimes \overline{\beta_1 \otimes \beta_2^{eq} + W_{1,2}} \\ \beta^{eq} &= \beta_1^{eq} \otimes \beta_2^{eq} \otimes \beta_3\end{aligned}$$

The above method is also illustrated in Figure 6. By expanding the expression of β_1^{eq} we obtain the following:

$$\beta_1^{eq} = \beta_1 \otimes \overline{\beta_1 \otimes \beta_2 \otimes \overline{\beta_2 \otimes \beta_3 + W_{2,3}} + W_{1,2}}\tag{6}$$

Equation (6) includes a nested SAC. Even assuming the simplest case, i.e., that service curves β_i are all rate-latency curves, the innermost SAC yields an UPP staircase function. The outer SAC must then be computed on a curve of this type, which is \mathcal{NP} -hard.

This method can be generalized to a tandem of n nodes, as:

$$\begin{aligned}\beta_{n-1}^{eq} &= \beta_{n-1} \otimes \overline{\beta_{n-1} \otimes \beta_n + W_{n-1,n}} \\ \beta_i^{eq} &= \beta_i \otimes \overline{\beta_i \otimes \beta_{i+1}^{eq} + W_{i,i+1}} \\ \beta^{eq} &= \bigotimes_{i=1 \dots n-1} \beta_i^{eq} \otimes \beta_n\end{aligned}\tag{7}$$

This method of analysis (henceforth: the *exact method*) therefore requires $O(n)$ nested SACs for a tandem of n nodes. All (except possibly one) are SACs of UPP curves. Therefore, despite the apparent conciseness of (7), computing β^{eq} via this method is infeasible in practice.

In [27], a property was proved that lower bounds β_i^{eq} with a *convolution of SACs*:

$$\beta_i^{eq'} = \beta_i \bigotimes_{j=i}^{n-1} \overline{\beta_j \otimes \beta_{j+1} + W_{j,j+1}}\tag{8}$$

Then, an end-to-end service curve can be computed as:

$$\begin{aligned}\beta^{eq'} &= \bigotimes_{i=1}^{n-1} \beta_i^{eq'} \otimes \beta_n \\ &= \beta_1^{eq'} \otimes \beta_2^{eq'} \otimes \dots \otimes \beta_{n-1}^{eq'} \otimes \beta_n \\ &= \beta_1 \otimes \bigotimes_{i=1 \dots n-1} \overline{\beta_i \otimes \beta_{i+1} + W_{i,i+1}} \\ &\quad \otimes \beta_2 \otimes \bigotimes_{i=2 \dots n-1} \overline{\beta_i \otimes \beta_{i+1} + W_{i,i+1}} \otimes \dots \otimes \beta_n \\ &= \bigotimes_{i=1 \dots n} \beta_i \otimes \bigotimes_{i=1 \dots n-1} \overline{\beta_i \otimes \beta_{i+1} + W_{i,i+1}}\end{aligned}\tag{9}$$

The above is a consequence of each $\overline{\beta_i \otimes \beta_{i+1} + W_{i,i+1}}$ being sub-additive, thus $f \otimes f = f$. Authors of [27] prove that:

$$\beta_i^{eq} \geq \beta_i^{eq'} \quad \forall i = 1 \dots n-1$$

From the above, since convolution is isotonic, it follows that:

$$\beta^{eq} \geq \beta^{eq'}\tag{10}$$

Computing $\beta^{eq'}$ via (9) (henceforth: the *approximate method*) is computationally more tractable – if all the SCs β_i are rate-latency – because it does away with nested SACs. However, it still requires one to compute $O(n)$ convolutions of UPP curves.

III. SYSTEM MODEL AND PROBLEM FORMULATION

Consider a flow traversing a tandem network of n flow-controlled nodes. Each node i has a rate-latency service curve $\beta_i = \beta_{\theta_i, R_i}$. After node i , $i < n$, there is a flow control window $W_{i,i+1}$. We initially assume that the flow-control is instantaneous, and implemented as described in Section II-B. We will come back to this issue at the end of this section. Our goal is to compute the end-to-end service curve of the above tandem network. This will allow one to compute a bound on the end-to-end delay and backlog, if the flow itself has an arrival curve. We want to be able to do this efficiently.

We first show that computing the end-to-end service curve, whether the exact or the approximate one, incurs representation explosion and may require very long computation times, even when n is small (e.g, three nodes).

We do this using a four-hop tandem of flow-controlled nodes as an example. We assume that the node parameters are those in Table I. We need to use two different sets of parameter values to better highlight the issues – and, later, the impact of the optimizations. In fact, the length and/or feasibility of the computations do depend on the parameter values. We found that a setting that can be solved with the exact method is often trivial with the approximate one, and a setting that is hard with the approximate method is often unfeasible with the exact one.

We attempt to compute the end-to-end equivalent service curves, via the exact and approximate methods, using the algorithms described in [25], on a desktop PC equipped with an Intel Core i9-9900, 16 GB of DRAM @3200 MHz, Windows 10 (the above system, included the software we run, is described in more detail in Section V).

We report computational results in, respectively, Table II and Table III, where we highlight both the representation size of the results and the time it takes to compute it. The alert reader will notice that the results reported in the tables are intermediate results towards the equivalent end-to-end service curves via Equation (7) and Equation (9), respectively. We cap computation

TABLE I
PARAMETERS OF THE EXAMPLE TANDEM NETWORK

i	Exact			Approximate		
	β_i delay	β_i rate	$W_{i,i+1}$	β_i delay	β_i rate	$W_{i,i+1}$
1	5	8	3	15	21	23
2	7	11	7	17	30	29
3	4	12	3	27	7	20
4	5	1		20	21	

TABLE II
COMPUTATIONAL RESULTS, EXACT METHOD

comp. time of $\overline{\beta_2 \otimes \beta_3^{eq} + W_{2,3}}$	6 h 24 m
$N(\beta_2 \otimes \beta_3^{eq} + W_{2,3}) \rightarrow N(\beta_2 \otimes \beta_3^{eq} + W_{2,3})$	10 \rightarrow 10600
comp. time of $\overline{\beta_1 \otimes \beta_2^{eq} + W_{1,2}}$ (s)	> 24 h
$N(\beta_1 \otimes \beta_2^{eq} + W_{1,2}) \rightarrow N(\beta_1 \otimes \beta_2^{eq} + W_{1,2})$	unknown

TABLE III
COMPUTATIONAL RESULTS, APPROXIMATE METHOD

comp. time of $\overline{\beta_{1,3} = \beta_1 \otimes \beta_2 + W_{1,2} \otimes \beta_2 \otimes \beta_3 + W_{2,3}}$	0.14 s
$N(\beta_1 \otimes \beta_2 + W_{1,2}), N(\beta_2 \otimes \beta_3 + W_{2,3}) \rightarrow N(\beta_{1,3})$	6, 6 \rightarrow 270
comp. time of $\overline{\beta_{1,4} = \beta_{1,3} \otimes \beta_3 \otimes \beta_4 + W_{3,4}}$	6 h 13 m
$N(\beta_{1,3}), N(\beta_3 \otimes \beta_4 + W_{3,4}) \rightarrow N(\beta_{1,4})$	270, 6 \rightarrow 1456

times at 24 hours.

The above results show that computation times are non trivial, and that state explosion does occur, even with the approximate method. As already outlined, we cannot abate these computation times by working on *compact domains*, as suggested in [29]. In fact, that method requires that the service curves involved are *super-additive*. In our model, the operands of these though convolutions are instead *sub-additive*, because they are the result of SACs. We are not aware of any method that allows one to limit the domains in this case.

A simple, but crude approach to compute an *approximated* end-to-end service curve would be to *lower bound* each resulting UPP curve with a rate-latency service curve. This approximation would have to be used after each SAC in (7), or for each term in (9). This would certainly make computations considerably faster, but may entail a considerable loss of accuracy.

We exemplify this using a simple UPP curve $\overline{\beta_{\theta,R} \otimes \beta_{\theta,R} + h}$. In this case, such lower bound would have $\theta_{lb} = \theta$, $R_{lb} = \frac{h}{\theta}$, and the error introduced by it is upper bounded by $\theta - \frac{h}{R}$. As shown in Figure 7, the impact of such error on the end-to-end delay depends on the characteristic of the input traffic. Notably, small messages would incur relatively larger penalty than large messages, and the loss in accuracy would be non negligible.

Our approach to gaining efficiency is to abate both the number and the computation time of *the convolutions of UPP curves*. This operation, in fact, lies at the core of both the exact and the approximate methods (recall that the SAC of an UPP curve can be computed as a convolution of elements, as explained in Section II-A). Reducing this number and making them as fast as possible is therefore going to make both methods more efficient. We do this *without introducing approximations*: our computations are always exact. In the next section, we show how we accomplish this, leveraging both state minimization and algebraic tools: first, we show that *minimizing the representation* R_f of the functions f involved in the operations may provide remarkable benefits. Then, we present three theorems that can be used to reduce the computation time of convolutions, leveraging sub-additivity of the operands.

Before introducing our contribution, we spend a few words discussing the generality of our model. With flow-controlled networks, different models can be envisaged as far as:

- 1) the exact place where flow-control stops traffic when the flow control window is closed, w.r.t. to the service curve modelling the sending node. For example, this may be an input buffer of the sending node, or an output buffer instead. The alert reader can check that using one or the other will lead to slightly different expressions for both the exact and the approximate end-to-end service curves. However, they will still be of the same type as (7) and (9), respectively, i.e., with either nested SACs or convolutions of sub-additive UPPs. Therefore, any computation issue that we address throughout this paper will still be present;
- 2) whether or not the return path, i.e., the flow-control credit feedback, is instantaneous. Depending on how such feedback is implemented, other models may, for instance, include a service curve on the return path as well. Again, this does not change the structure of the expressions that we seek to compute efficiently.

Thus, only the model of Figure 4 will be considered henceforth for simplicity.

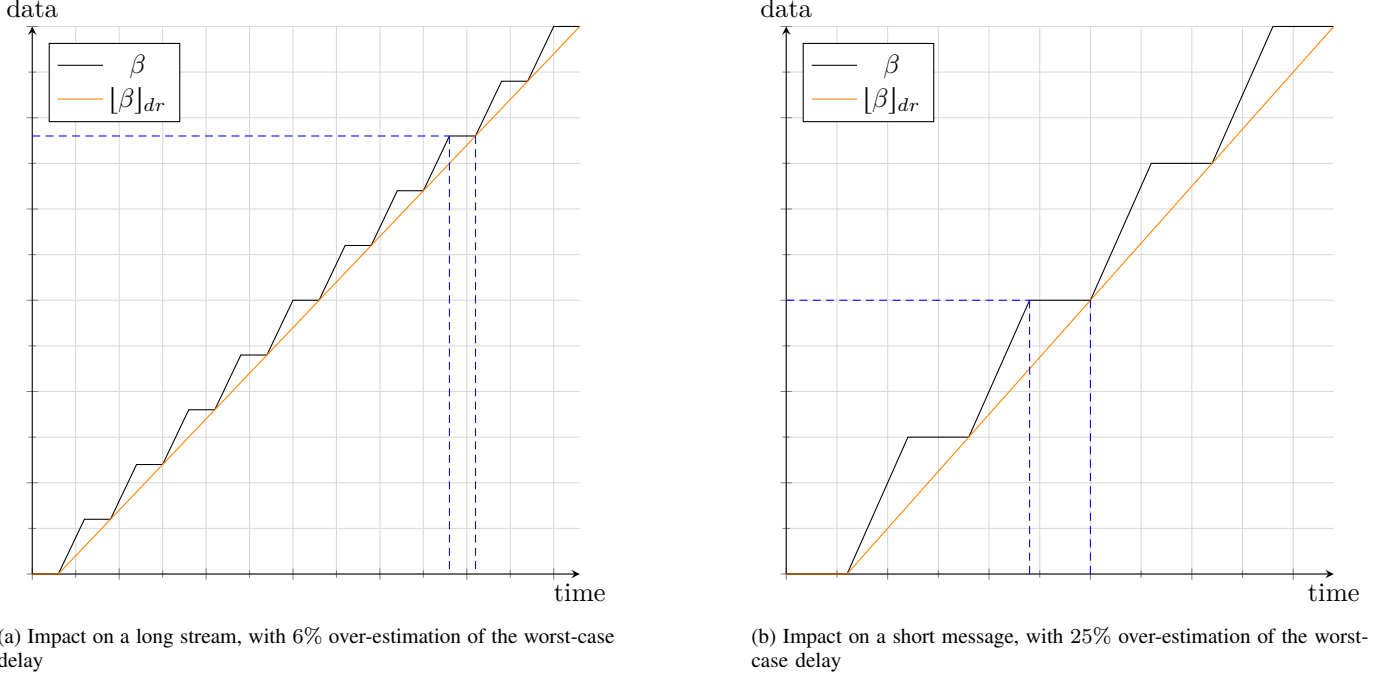


Fig. 7. Delay overestimation introduced by lower-bounding an UPP via a rate-latency curve

IV. CONTRIBUTION

We present our two contributions separately. First, we show how to minimize the representation of a function, using an inexpensive algorithm. Then, we show theorems that reduce the cost of convolutions.

A. Representation minimization

As discussed, given a representation $R_f = (S, T, d, c)$ of function f , its cardinality $N(S)$ is the main factor for the algorithmic complexity of operations involving it. A first way to abate computation times is therefore to find the *minimal* representation of f .

We say that two representations R_f and R_g are *equivalent* if they represent the same function, i.e., $f(t) = g(t) \forall t \geq 0$. A *minimal* representation R_f is such that, given any equivalent representation R_f , then $N(\tilde{S}) \leq N(S)$.

Unfortunately, the generic algorithms for operations on UPP curves (described in [25], [26] and recalled in Section II-A and in the Appendix) do not yield minimal representations, even when the representations of their operands are minimal. The steps described in Section II-A, in fact, compute the smallest values that can be formally proved to be valid *a priori*, with no knowledge of the shape of the result. These values can be much larger than those of a minimal representation.

A simple example is given in Figure 8. Starting from the parameters of the operands, the algorithm computes $T = 7$ for the result. However we can see that the result is actually a rate-latency curve that can be described with $T = 5$. This phenomenon – that we have just exemplified using a minimum operation – affects convolution as well, and it is especially impactful when many convolutions are required, such as in a SAC or in Equation (8), where the result of one is in fact the operand of the next. In fact, we recall that the cost of the convolution is quadratic with the size of the extended representations of the operands (Section II).

Note that there is no efficient way – that we know of – to predict the minimum representation *a priori*, i.e., before the operation is computed. This is basically because the result depends on unpredictable numerical properties of the operands (e.g., the segment endpoints). We therefore introduce an algorithm to minimize the representation *a posteriori*, i.e., after the result of the operation has been computed. We will show later that minimization is computationally cheap, and may yield considerable speedups.

For the following discussion, it will be useful to define an umbrella term for the points of a function in which linear behavior is broken. We say that f has a *breakpoint* in t_b if at least one of the following is true:

- f has a discontinuity in t_b
- the rates of f in t_b^- and t_b^+ are different

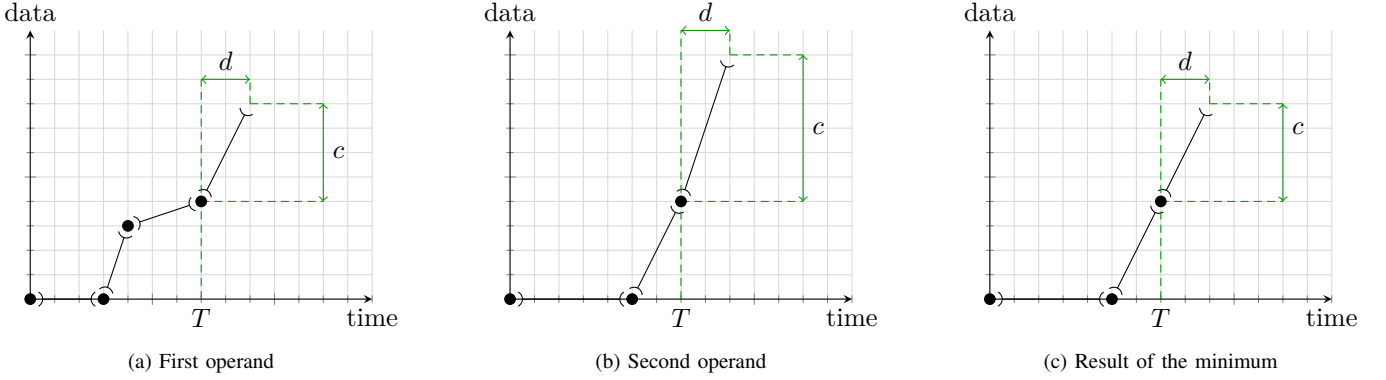


Fig. 8. Example of non-minimal result of a minimum operation

A first thing to do is to ensure that the sequence in a representation is *well-formed*. We say that S is a *well-formed* sequence if any point in S corresponds to a breakpoint of f . In other words, in a *well-formed* sequence there are no *unnecessary points*².

As we anticipated, the generic algorithms for minimum and convolution may not yield well-formed sequences, even when the sequences of their operands are well-formed. However, recovering well-formedness only takes a simple $O(N(S))$ check of the resulting sequence S , to find segment-point-segment triplet that can be merged, i.e., replaced with a single segment. From now on, we will therefore assume that sequences are well-formed, without loss of generality.

Ensuring that the transient and pseudo-periodic parts of a representation are minimal is instead less obvious. We present a minimization algorithm consisting of two phases:

- factorization of the pseudo-period;
- reduction of the transient.

1) *Factorization of the pseudo-period*: We first consider the simplest case where f is ultimately affine, i.e., the pseudo-periodic part consists of a simple half-line. Such half-line can be described by any couple $d', c' \mid c'/d' = c/d$. Whatever the chosen values, S_f^P will only consist of a point of value $f(T)$ and a segment of length d and slope c/d . This just means that there is nothing to do in this case.

If, instead, f is not ultimately affine, one may observe that, given any $k > 1, k \in \mathbb{N}$, we can find an equivalent representation of f using $d_2 = k \cdot d$ and $c_2 = k \cdot c$. We also observe that this is the only possible case: it would be impossible to find two representations, having S_f^P and $S_f^{P'}$ with time lengths $l > l' \mid l/l' \notin \mathbb{N}$, that are also equivalent. In fact, if there is a smaller representation $S_f^{P'}$, i.e., $\exists d', c' \mid f(t + k \cdot d') = f(t) + k \cdot c' \forall t \geq T, k \in \mathbb{N}$, then it must be $d/d' = c/c' = p \in \mathbb{N}$.

Thus, we set to finding these $p \in \mathbb{N}$, which we call *divisors* of S_f^P , which is what allows us to reduce it as exemplified in Section IV-A1.

Now, if f is not ultimately affine, it must have at least a breakpoint in each pseudo-period, i.e., at least one in $]T, T + d]$. Furthermore, let $b \in \mathbb{N}$ be the number of breakpoints of f in $]T, T + d]$. It follows that, if $\exists p$ as defined above, then p is a divisor of b .

This allows us to formulate an algorithm that minimizes S_f^P to optimality:

- 1) Count b as the number of breakpoints of f in $]T, T + d]$;
- 2) Find the prime factorization of b ;
- 3) Exhaustively test the prime factors of b against S_f^P , to find which ones are also divisors of S^P .

Counting the breakpoints of f is a simple $O(N(S_f^P))$ check. To find the prime factorization of b , we will need the prime numbers in $2 \dots \sqrt{b}$. Computing primes until a given x is something that can be done offline – we use an offline list of 1000 primes in our implementation, which is enough for periods exceeding 62 millions. Lastly, testing if a prime factor p is a divisor of S_f^P entails a linear comparison between its parts. Let k be the number of prime divisors of b , then the complexity of this last step is $O(k \cdot N(S_f^P))$.

2) *Reduction of transient*: In a non-minimal representation, the period start T can be overrated, making the transient part longer than strictly necessary. *Transient reduction* aims at removing this excess transient by bringing forward the period start. We exemplify this process starting from the representation in Figure 10.

As a first step, which we call *by period*, we check if the transient contains sequences equivalent, minus due offsets, to the pseudo-period itself – and remove them, in case. In the example we can see that the representation is equivalent to the one in Figure 11.

²An exception must be made at T , where a point has to be inserted regardless, marking the end of the transient and the beginning of the periodic part, because this simplifies the implementation. Such an exception has no impact on the rest of our discussion.

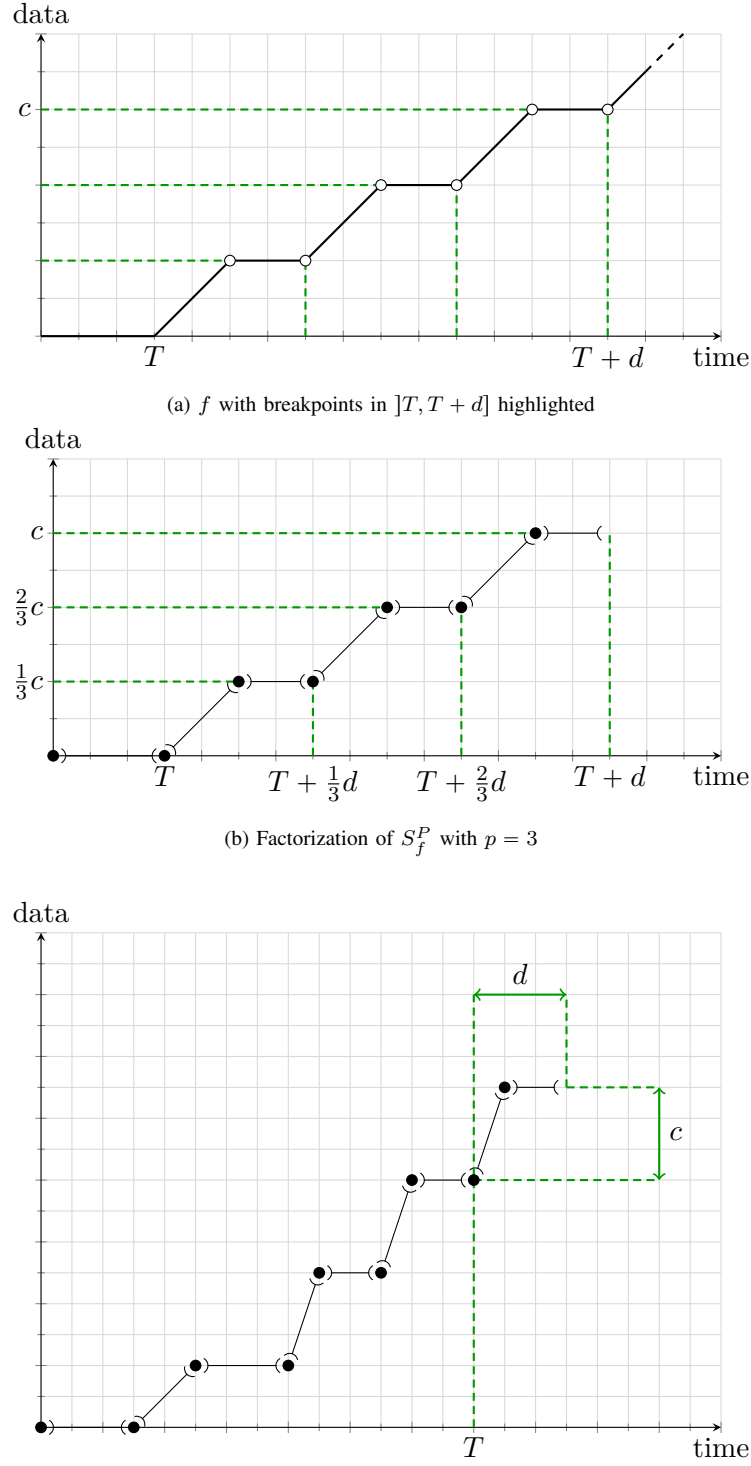


Fig. 10. Example of a non-minimal representation

We can obtain this result algorithmically by comparing the pseudo-period sequence in $[T, T + d[$ with the transient sequence immediately before, i.e., in $[T - d, T[$. If the two are equivalent, minus an offset c , than the period start can be brought forward to $T - d$, while the other parameters stay the same. This operation removes a pseudo-period's worth of segments from the representation.

We repeat this process iteratively until the comparison fails. The end result is a reduction of the representation by a number of periods $k \in \mathbb{N}$, and an earlier period start $T' = T - k \cdot d$.

As a second step, which we call *by segment*, we test if *parts* of a pseudo-period, instead of whole periods, can be found at

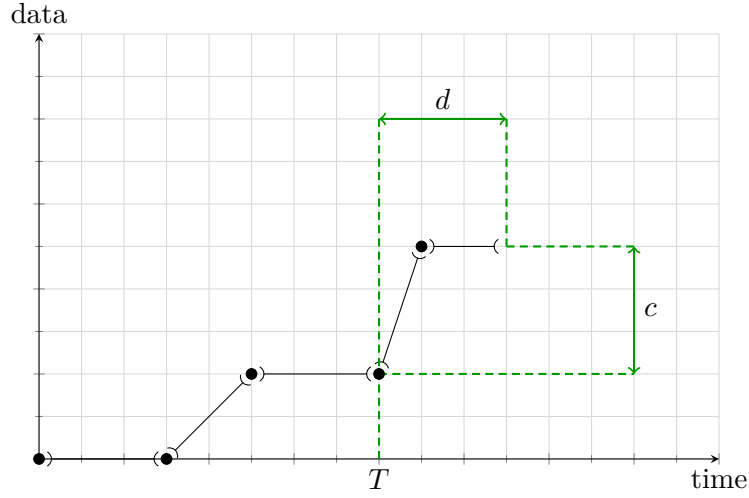


Fig. 11. Representation reduced by a whole number of periods

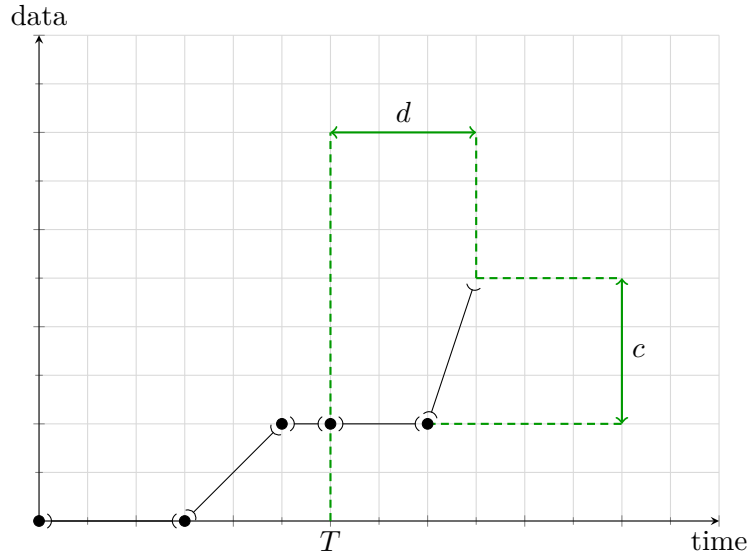


Fig. 12. Representation reduced by a segment, altering the pseudo-period sequence

the right end of the transient part. In the example we can see that the representation is equivalent to the one in Figure 12. We can algorithmically obtain this result by comparing the last segment of the pseudo-period, say $[T + d - l, T + d]$, thus of length l , with the transient segment of the same length immediately before the period start, thus in $[T - l, T]$. If the two are equivalent, minus an offset c , then the period start is brought forward to $T - l$, while the other parameters stay the same. While this appears close to the *by period* step, an important difference is that the pseudo-periodic sequence needs also be altered as a result.

An edge case of this technique is that of a curve having a half-line period. When checking for possible reduction of the representation, one should only check if the tail of the transient is aligned with the half-line, instead of using the values of d and c to attempt a comparison.

The above steps are repeated until no further change can be made, thus when S_f^T and T are the smallest possible. When done after the period factorization, the overall description will thus be the minimal one.

As the linear comparisons involve, at most, the entire S_f^T , the cost of this algorithm is $O(N(S_f^T))$. Thus the cost of the overall minimization algorithm is $O(N(S_f^T) + k \cdot N(S_f^P))$.

With reference to the example presented in Section III, we repeated the same computations, this time adding representation minimization in between each operation (both minima and convolutions).

The new results are in Table IV and Table V, which highlight both speedups and reductions in representation size up to three

orders of magnitude.

An important aspect that links both is that a larger representation size translates directly to a higher memory occupancy during computations. As the occupied memory approaches the maximum allowed by the computer system, the performance is also affected. We do believe that the reason why some SACs do not terminate with the exact method is that they end up occupying all the available memory, hence disk swaps start kicking in.

TABLE IV
COMPUTATIONAL RESULTS, EXACT METHOD

	unoptimized results	with minimization
comp. time of $\beta_2 \otimes \beta_3^{eq} + W_{2,3}$	6 h 24 m	6 s
$N(\beta_2 \otimes \beta_3^{eq} + W_{2,3}) \rightarrow N(\beta_2 \otimes \beta_3^{eq} + W_{2,3})$	10 → 10600	10 → 10
comp. time of $\beta_1 \otimes \beta_2^{eq} + W_{1,2}$ (s)	24 h	13 s
$N(\beta_1 \otimes \beta_2^{eq} + W_{1,2}) \rightarrow N(\beta_1 \otimes \beta_2^{eq} + W_{1,2})$	unknown	14 → 6

TABLE V
COMPUTATIONAL RESULTS, APPROXIMATE METHOD

	unoptimized results	with minimization
comp. time of $\beta_{1,3} = \beta_1 \otimes \beta_2 + W_{1,2} \otimes \beta_2 \otimes \beta_3 + W_{2,3}$	0.14 s	0.11 s
$N(\beta_1 \otimes \beta_2 + W_{1,2}), N(\beta_2 \otimes \beta_3 + W_{2,3}) \rightarrow N(\beta_{1,3})$	6, 6 → 270	6, 6 → 42
comp. time of $\beta_{1,4} = \beta_{1,3} \otimes \beta_3 \otimes \beta_4 + W_{3,4}$	6 h 13 m	13.47 s
$N(\beta_{1,3}), N(\beta_3 \otimes \beta_4 + W_{3,4}) \rightarrow N(\beta_{1,4})$	270, 6 → 1456	42, 6 → 6

B. Efficient convolutions of sub-additive functions

In a convolution the resulting period grows like the *lcm* of the period of the operands, and the complexity of the by-sequence algorithm is superquadratic with the length of the extended sequences. Thus, it is possible to find instances where a *single* convolution may take very long.

It is however possible to leverage sub-additivity to reduce the complexity of the convolution. To the best of our knowledge, this has never been observed before.

We first observe that *dominance* can be leveraged to abate the complexity of convolutions. We say that g *dominates* f if $g(t) \geq f(t) \forall t \geq 0$. In this case:

Theorem 1 (Convolution of sub-additive functions with dominance). *Let f and g be UPP functions such that*

- $f(0) = g(0) = 0$
- $g(t) \geq f(t) \forall t$
- f is sub-additive

Then $f \otimes g = f$

Proof. Being sub-additive, $f(u) + f(s) \geq f(u + s) \forall u, s$.

Then for any $t = u + s$, $f(u) + g(s) \geq f(u) + f(s) \geq f(t)$.

Thus $(f \otimes g)(t) = \inf_{u+s=t} \{f(u) + g(s)\} = f(t) + g(0) = f(t)$

□

In order to apply this theorem algorithmically, we first need to compare the two functions f and g . Dominance can be verified by checking equivalent statements $f == \min(f, g)$, $g == \min(f, g)$. Both the minimum and the equivalence check have linear costs as discussed in Section II-A. When either is true, Theorem 1 allows us to bypass the convolution altogether, which is instead superquadratic. Note that this theorem (as well as the following one) requires only the *dominated* function f to be sub-additive, whereas the dominant function g can have any shape, as long as $g(0) = 0$. However, given our hypotheses, both operands of convolutions are always sub-additive by construction.

When dominance does not hold, we can test a weaker property, *asymptotic dominance*. We say that g *dominates* f *asymptotically* if $g(t) \geq f(t) \forall t \geq \bar{t} > 0$. Note that $\rho_g > \rho_f$ is a sufficient conditions for this to occur, but not a necessary one. In this case, we can resort to a "simpler" convolution as follows:

Theorem 2 (Convolution of sub-additive functions with asymptotic dominance). *Let f and g be UPP functions such that*

- $f(0) = g(0) = 0$
- $g(t) \geq f(t) \forall t \geq t^*$
- f is sub-additive

Let $g = g_a \wedge g_b$ be a decomposition of g where g_a is defined in $[0, t^*]$ and g_b is defined in $[t^*, +\infty[$. Both g_a and g_b have value $+\infty$ outside the above intervals.

Then $f \otimes g = f \otimes g_a \wedge f$

Proof. Decompose g as per the hypothesis. Then:

$$\begin{aligned} f \otimes g &= f \otimes (g_a \wedge g_b) \\ &= f \otimes g_a \wedge f \otimes g_b \end{aligned}$$

For the latter part, we observe that:

$$\begin{aligned} g_b(t) &= +\infty \quad \forall t \in [0, t^*] \\ g_b(t) &\geq f(t) \quad \forall t > t^* \\ \Rightarrow g_b &\geq f \quad \forall t \end{aligned}$$

We can thus apply Theorem 1, for which $f \otimes g_b = f$. Thus:

$$\begin{aligned} f \otimes g &= f \otimes g_a \wedge f \otimes g_b \\ &= f \otimes g_a \wedge f \end{aligned}$$

□

If g dominates f only asymptotically, then f is above g at some point, but will eventually fall below it. Thus $\exists \bar{t}^* \rightarrow f(t) \leq g(t) \quad \forall t \geq \bar{t}^*$, and by algorithmic construction of $f \wedge g$ we can say that $T_{f \wedge g}$ is in fact such \bar{t}^* ³.

Thus we can apply Theorem 2, and compute $f \otimes g$ by:

- Computing $h = f \otimes g_a$. Since $g_a(t) = +\infty \quad \forall t \geq t^*$, computing this convolution will involve extension with $d = d_f$ rather than $\text{lcm}(d_f, d_g)$, thus reducing the cost by avoiding long period extensions.
- Computing $f \otimes g = h \wedge f$. Being a minimum, it has a linear cost, but again $d = \text{lcm}(d_h, d_f) = \text{lcm}(d_f, d_f) = d_f$, hence the number of operations is greatly reduced.

Thus, the main benefit of applying Theorem 2 lies in dispensing with the extension of the representation of f and g over a possibly very long period $d = \text{lcm}(d_f, d_g)$.

If neither of the above theorems can be applied, then:

- $\rho_f = \rho_g$;
- f and g intersect an infinite number of times, because they have intersections in their pseudo-periodic parts.

In this case, we can resort to the following property:

Theorem 3 (Convolution of sub-additive functions as self-convolution of the minimum). *Let f and g be non-negative sub-additive functions such that $f(0) = g(0) = 0$.*

Then $f \otimes g = (f \wedge g) \otimes (f \wedge g)$.

Proof. We recall that:

- if f is sub-additive with $f(0) = 0$, $f \otimes f = f$ ([9, Corollary 3.1.1])
- $f \wedge g \geq f \otimes g$ ([9, page 113])

Then

$$\begin{aligned} (f \wedge g) \otimes (f \wedge g) &= (f \otimes f) \wedge (f \otimes g) \wedge (g \otimes f) \wedge (g \otimes g) \\ &= f \wedge (f \otimes g) \wedge (f \otimes g) \wedge g \\ &= f \wedge g \wedge (f \otimes g) \\ &= (f \wedge g) \wedge (f \otimes g) \\ &= f \otimes g \end{aligned}$$

□

To exploit this theorem, we would first need to compute $f \wedge g$. However, this computation is also a prerequisite for testing Theorem 1, which one would try first anyway. Theorem 3 transforms a convolution into a *self-convolution*. Self-convolutions can

³The alert reader may note that this is not true if *transient reduction* is applied to $f \wedge g$ – we indeed backup $T_{f \wedge g}$ beforehand.

be computed more efficiently than standard convolutions. In fact, we can bypass more than half of the elementary convolutions within the by-sequence algorithm, as per the following properties:

Property 3 (Avoiding duplicates in self-convolutions). *A self-convolution $f \otimes f$ can be computed through a single by-sequence convolution with $S_f^D, D = [0, T_f + 2 \cdot d_f]$.*

Since the by-sequence convolution $S_f^D \otimes S_f^D$ is symmetrical, we can reduce the elementary convolutions to

$$\frac{n^2 - n}{2} < n^2,$$

where $n = N(S_f^D)$

Proof. Since the two operands of the convolution have the same ρ_f , from [25] we know that:

- $T = T_f + T_f + d = 2 \cdot T_f + d$ ⁴
- $d = \text{lcm}(d_f, d_f) = d_f$
- $c = \rho \cdot d = c_f$

Consider then $S_f^D, D = [0, T + \cdot d_f]$ and its componing elements

$$\begin{aligned} S_f^D &= e_0 \wedge e_1 \wedge \cdots \wedge e_n \\ S_f^D \otimes S_f^D &= \bigwedge_{e_i, e_j} e_i \otimes e_j \rightarrow n^2 \text{ elementary convolutions} \end{aligned}$$

However, convolution being commutative, many of these are computed twice, e.g., $e_1 \otimes e_2, e_2 \otimes e_1$. We can avoid this through:

$$\begin{aligned} S_f^D \otimes S_f^D &= \bigwedge_{e_i, e_j: i, j \in [0..n-1]} e_i \otimes e_j \\ &= \bigwedge_{e_i, e_j: i, j \in [0..n-1], i < j} e_i \otimes e_j \wedge \bigwedge_{e_i: i \in [0..n-1]} e_i \otimes e_i, \end{aligned}$$

which results in $n + n - 1 + \cdots + 1 = \frac{n^2 - n}{2}$ elementary convolutions. \square

Therefore, in a self-convolution (such as the one of Theorem 3) one can halve the number of elementary convolutions. On top of that, a further improvement is warranted by the following property:

Property 4 (Reducing the number of convolutions by element coloring). *Let $h = f \wedge g$ and D be domain necessary to compute $h \otimes h$.*

Consider the decomposition of S_h^D in n elements e_i , and consider each element to be colored based on the function it belongs to, which is defined as:

- e_k defined in domain D_k
- $e_k(t) = f(t) \forall t \in D_k \rightarrow \text{color}(e_k) = f$
- otherwise, $\text{color}(e_k) = g$

Then, we can omit all convolutions between e_i, e_j where $\text{color}(e_i) = \text{color}(e_j)$.

Proof. Consider the elementary convolution between points $p_a = (t_a, v_a)$ and $p_b = (t_b, v_b)$, such that $\text{color}(p_a) = \text{color}(p_b) = f$.

By the sub-additivity of f , $f(t_a + t_b) \leq v_a + v_b$. Since we assumed $f(0) = g(0) = 0$, then $h(0) = 0$. Consider then the value of $(h \otimes h)(t_a + t_b)$.

If $h(t_a + t_b) = f(t_a + t_b)$, then

$$\begin{aligned} (h \otimes h)(t_a + t_b) &\leq h(0) + h(t_a + t_b) \\ &= f(t_a + t_b) \\ &\leq v_a + v_b \end{aligned}$$

If, instead, $h(t_a + t_b) = g(t_a + t_b)$, we can say

$$\begin{aligned} (h \otimes h)(t_a + t_b) &\leq h(0) + h(t_a + t_b) \\ &= g(t_a + t_b) \\ &\leq f(t_a + t_b) \\ &\leq v_a + v_b \end{aligned}$$

⁴When combined with Theorem 3, we can use $T = \min(2 \cdot T_{f \wedge g}, T_f + T_g)$

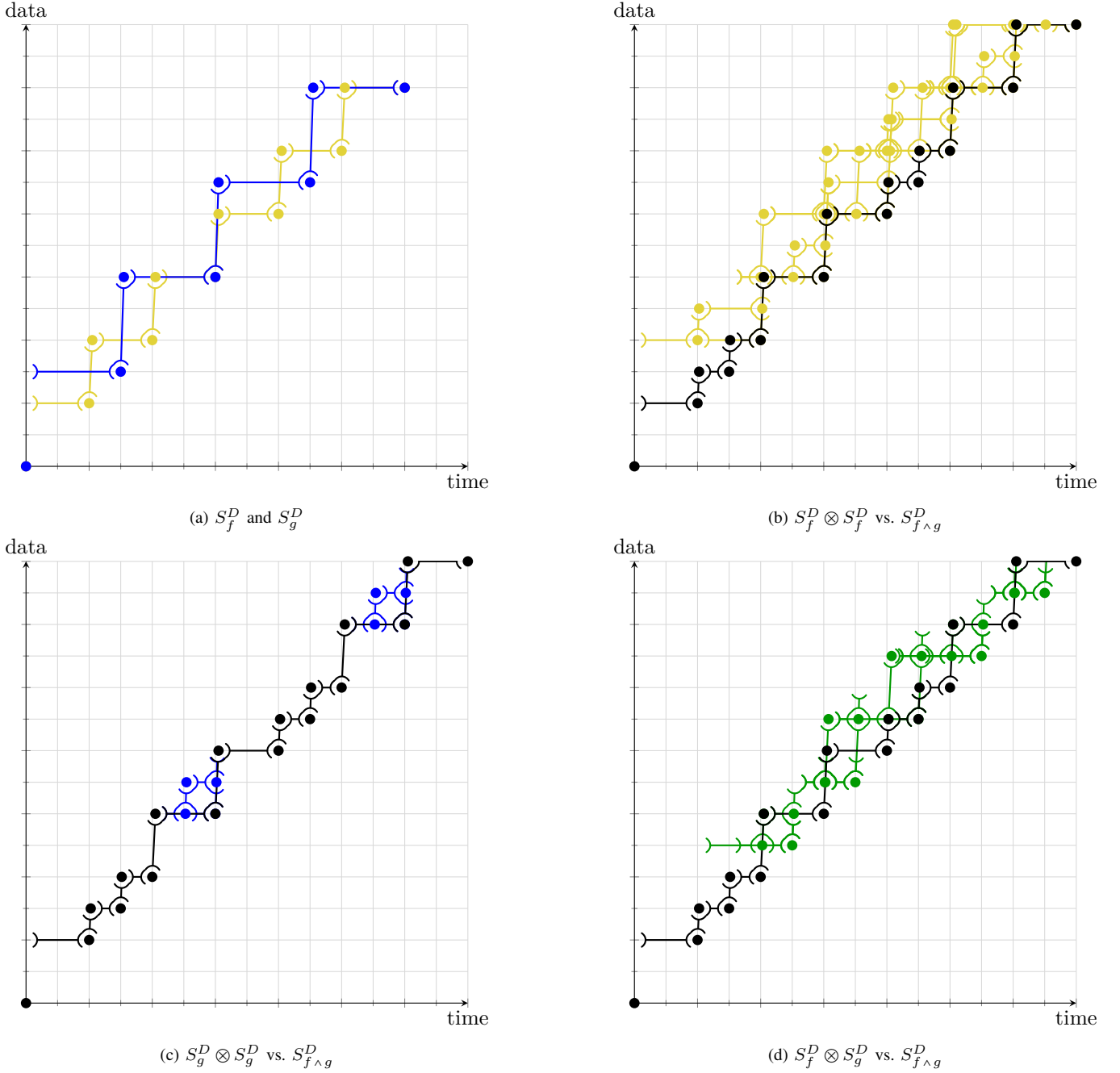


Fig. 13. Coloring example

Therefore, computing $p_a \otimes p_b$ is useless for the purpose of computing $h \otimes h$.

The alert reader will notice that the same argument extends to the case of convolutions of different elements (e.g., segment and point, segment and segment), basically because segments can be considered one point at a time. We thus omit to repeat the proof. \square

The idea behind Property 4 can be visualized through the example in Figure 13. Given f and g (Figure 13a), Figure 13b and Figure 13c show how no convolution between elements of the same color provide any new information over $f \wedge g$. Instead, in Figure 13d we see how convolutions of elements of different color may yield points and segments below $f \wedge g$.

The above two properties allow one to make the computation of $(f \wedge g) \otimes (f \wedge g)$ as efficient as possible, skipping many elementary convolution. However, it remains to be seen whether computing the above is faster than computing $f \otimes g$ directly. Our results, reported in Section V-A4, show that this is indeed the case in the vast majority of cases: the ensuing time reduction ranges from sizeable percentages to $10\times$. Counterintuitively, this is not due to a reduction in the number of elementary convolutions (which is instead of the same order of magnitude in the two cases, despite the optimizations of

Property 3 and Property 4). Rather, it is due to the different topological properties of the ensuing elements in the two cases. A thorough discussion of this phenomenon is reported in Section V-A4.

With reference to the example presented in Section III, we repeated the same computations, this time exploiting also the theorems proved in this section.

The new results are in Table VI and Table VII, which highlight further reductions in computation time.

TABLE VI
COMPUTATIONAL RESULTS, EXACT METHOD

	w/o optimizations	minimization	minimiz. + Th. 1,2,3
comp. time of $\overline{\beta_2 \otimes \beta_3^{eq} + W_{2,3}}$	6 h 24 m	6 s	0.47 s
$N(\beta_2 \otimes \beta_3^{eq} + W_{2,3}) \rightarrow N(\beta_2 \otimes \beta_3^{eq} + W_{2,3})$	10 → 10600	10 → 10	10 → 10
comp. time of $\beta_1 \otimes \beta_2^{eq} + W_{1,2}$ (s)	> 24 h	13 s	0.18 s
$N(\beta_1 \otimes \beta_2^{eq} + W_{1,2}) \rightarrow N(\beta_1 \otimes \beta_2^{eq} + W_{1,2})$	unknown	14 → 6	14 → 6

TABLE VII
COMPUTATIONAL RESULTS, APPROXIMATE METHOD

	w/o optimizations	minimization	minimiz. + Th. 1,2,3
comp. time of $\beta_{1,3} = \beta_1 \otimes \beta_2 + W_{1,2} \otimes \beta_3 \otimes \beta_3 + W_{2,3}$	0.14 s	0.11 s	0.09 s
$N(\beta_1 \otimes \beta_2 + W_{1,2}), N(\beta_2 \otimes \beta_3 + W_{2,3}) \rightarrow N(\beta_{1,3})$	6, 6 → 270	6, 6 → 42	6, 6 → 42
comp. time of $\beta_{1,4} = \beta_{1,3} \otimes \beta_3 \otimes \beta_4 + W_{3,4}$	6 h 13 m	13.47 s	0.003 s
$N(\beta_{1,3}), N(\beta_3 \otimes \beta_4 + W_{3,4}) \rightarrow N(\beta_{1,4})$	270, 6 → 1456	42, 6 → 6	42, 6 → 6

V. PERFORMANCE EVALUATION

In this section, we first evaluate the impact of our findings by measuring the speedup that they yield with respect to the standard algorithms described in Section II-A, taken from [26]. Then, we show how our method allows one to analyze long tandems of flow-controlled nodes, and we compare the exact and approximate analysis methods as for efficiency and accuracy.

A. Computational results

We run our experiments on a desktop PC equipped with an Intel Core i9-9900, 16 GB of DRAM @3200 MHz, Windows 10. Our NC library is written in C# (.NET 6), and can exploit the PLINQ framework to easily parallelize and scale the algorithms in multicore processors. However, to minimize the perturbations and improve the fairness of comparisons, our experiments are run in single-thread mode. This allows us to obtain consistent time measurements: we verified that the execution times of independent replicas of the same experiment differ by fractions of percentage points. For this reason, confidence intervals are omitted. As numerical base type we introduce a *Rational* type, in which both numerator and denominator are represented using *System.Numerics.BigInteger*, which is an integer type with no upper or lower bounds. This comes at a performance cost over using 64-bit integers, but has the distinctive advantage of removing all issues with arithmetic overflow. Execution times are measured using the *System.Diagnostic.Stopwatch* class. When applying our optimizations, the execution times we measure also include those testing our hypotheses (e.g., dominance or asymptotic dominance).

In the experiments, we focus on convolutions between UPP curves in the form $\beta_{d,r,h} = \overline{\beta_{d,r} + h}$, where $\beta_{d,r}$ is a rate-latency curve, with latency d and rate r , and h is a constant function.

Parameters d, r, h are generated using a pseudo-random generator (*System.Random*) that produces integers between 1 and 1000. The resulting curves are further filtered in order to match the properties required by the theorems being tested. We analyze separately the speedup obtained with representation minimization and with the Theorems described in Section IV.

1) *Representation Minimization*: We now test the impact of representation minimization, described in Section IV-A. We compute $(\beta_a \otimes \beta_b) \otimes \beta_c$, where the three operands are randomly generated as described above. First, we computed the convolutions without any improvement. Then, we computed the same convolutions using representation minimization both on the results and in between any intermediate step: for instance, when we compute Equation (4), we minimize the result of each of the four partial convolutions. Note that the algebraic properties of Theorems 1 to 3 were not used in this study.

We first report in Figure 14 the reduction in the number of elements of the result. Each experiment is reported as a point on a cartesian plane (with logarithmic scales), whose vertical coordinate is the number of elements of the minimized result, and whose horizontal coordinate is the number of elements of the unoptimized one. The dashed line is the bisector, below which the state reduction is larger than 1×. This makes it easier to visualize the order of magnitude of the reduction, which is in

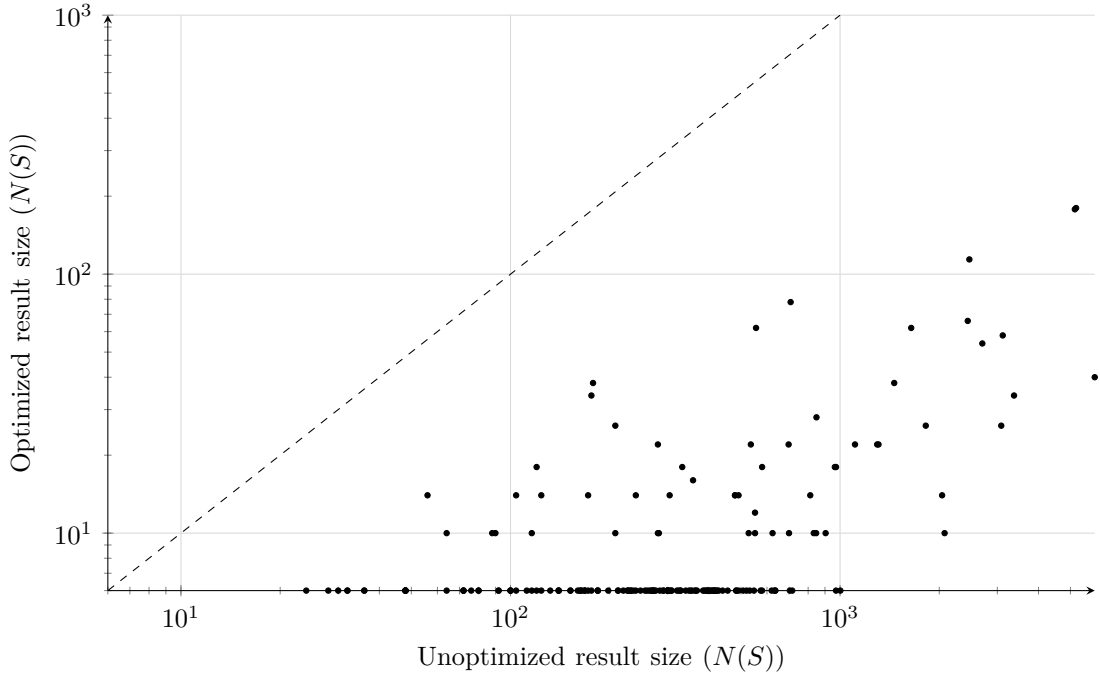


Fig. 14. Results for convolution between 3 sub-additive functions, with and without minimization

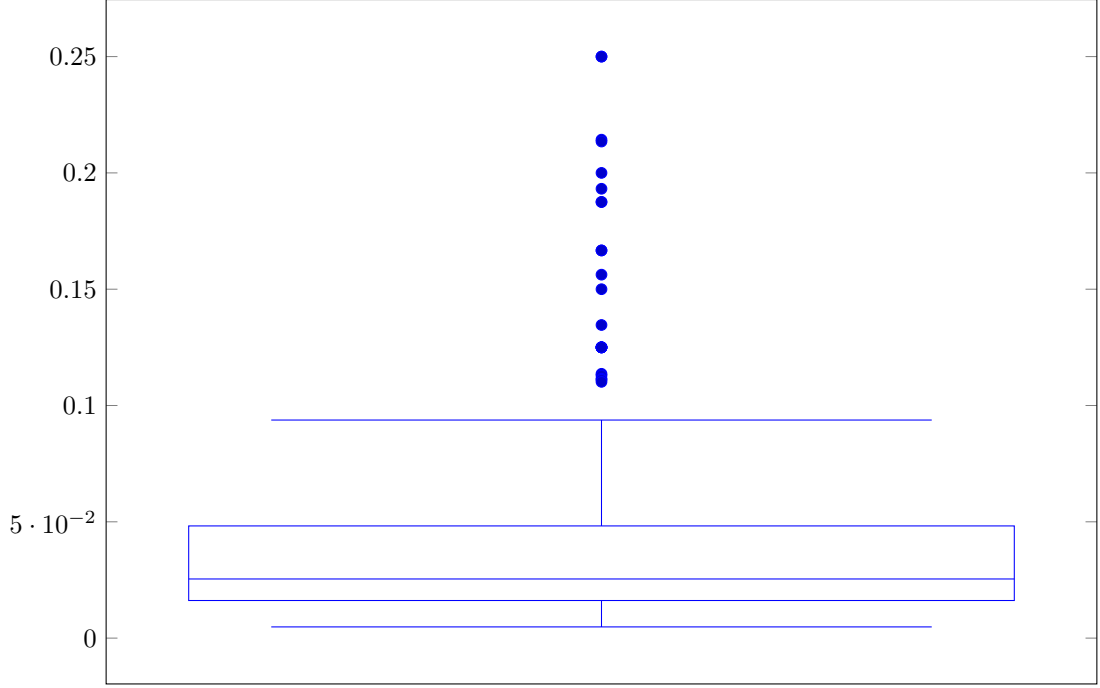


Fig. 15. Reduction of result cardinality for convolution between 3 sub-additive functions, with and without minimization

fact the horizontal (or vertical) distance between a point and the bisector. Figure 14 highlights state reductions of one to three orders of magnitude. A box plot of the state reduction is shown in Figure 15.

We have presented in Section IV-A an example where representation minimization also yielded a speedup of orders of magnitude. We therefore compare the running time of the above operations in Figure 16, which compares the optimized and unoptimized running times, and in Figure 17, where we report a box plot of the reduction in computation times.

Our results show that – while some gains are certainly there in most cases – a high reduction in the state occupancy does not always yield a similar reduction in computation times. The median time reduction is in the order of 10%. This can be explained by observing that the impact of *period factorization* on the *lcm* is variable. Consider for example two curves, f

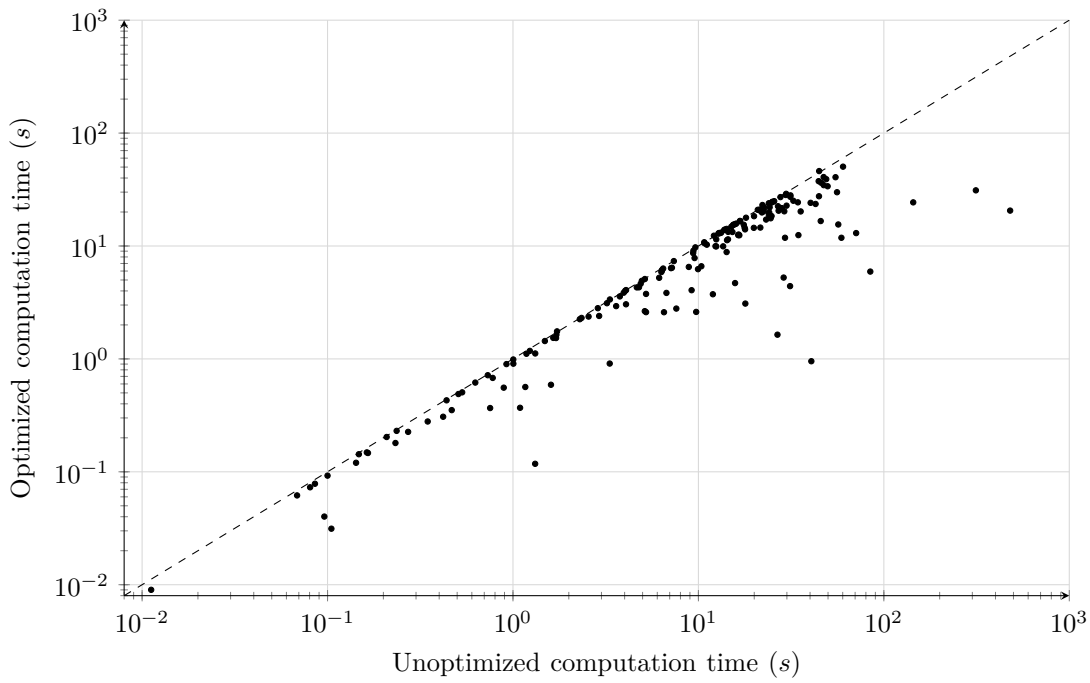


Fig. 16. Results for convolution between 3 sub-additive functions, with and without minimization

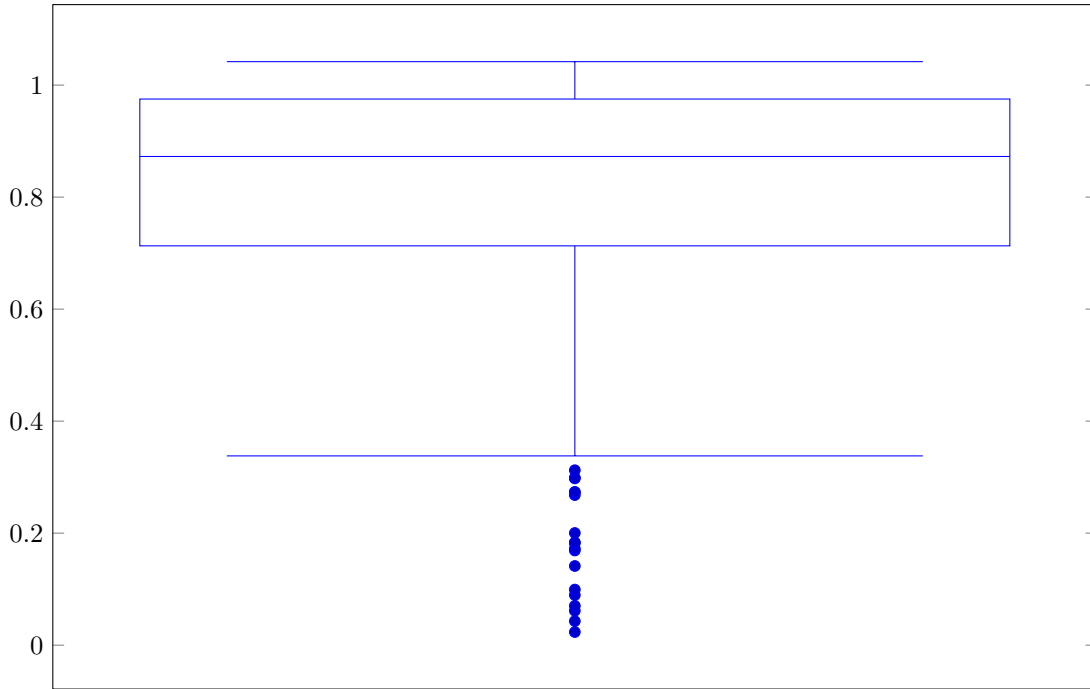


Fig. 17. Reduction of computation times for convolution between 3 sub-additive functions, with and without minimization

and g , and their respective representations with $d_f = 30$ and $d_g = 30$, such that by performing period factorization on these representations we obtain $d'_f = 5, d'_g = 6$. While the reduction in size is noticeable, the same cannot be said about computing $f \otimes g$, since $\text{lcm}(30, 30) = \text{lcm}(5, 6)$. Thus, the more substantial speedups are obtained when minimization succeeds in removing a common factor from both operands (e.g., factor 5 from both f and g). Note that these cases (to which the example of Section IV-A belongs) depend on numerical properties of the operands, hence are hard to obtain using random generation of the input (but not impossible – check the outliers at the bottom of Figure 17).

We stress that the most remarkable benefits of representation minimization lie in enabling the computation of SACs, hence the analysis of networks via the exact method. In this case, representation minimization is indispensable, since the complexity of

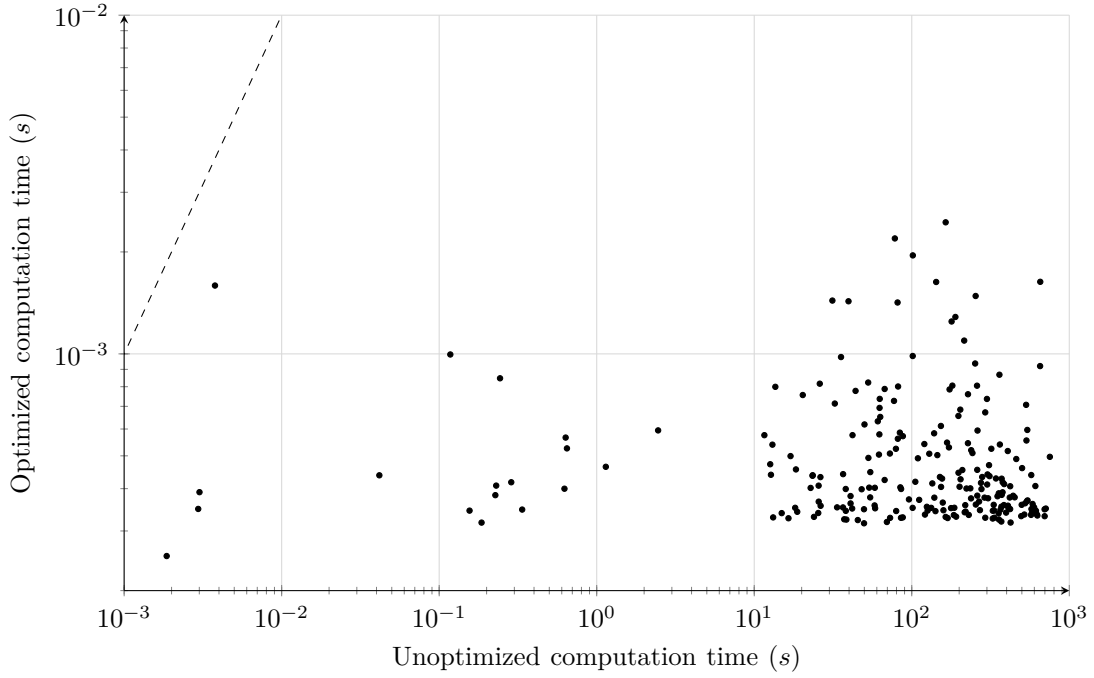


Fig. 18. Results for convolution between sub-additive functions with dominance

the SAC algorithm is exponential with the number of elements. Unfortunately, we are not able to produce a speedup figure for the SACs, since unoptimized SACs with random parameters hardly ever terminate at all.

On the other hand, the above experiments highlight that applying minimization always yields a significant size reduction, which helps with memory management; it yields at least a moderate time reduction, most of the times, and – even in the rare cases when it fails to provide a speedup – the time spent on applying it is negligible.

2) *Convolution of sub-additive functions with dominance:* We now test the impact of Theorem 1. We compute $\beta_{d_1, r_1, h_1} \otimes \beta_{d_2, r_2, h_2}$, where the operands are randomly generated and matching the hypotheses of Theorem 1. To make the comparison more insightful, we apply representation minimization, to all intermediate computations, in the baseline unoptimized algorithm, in these and the following experiments.

The benefits of using Theorem 1 can be seen in Figure 18, which clearly shows that most speedups are in the region of $10^5 \times$. In many cases the unoptimized convolution lasted more than 10 minutes, while the optimized version seldom lasted more than 1 ms. This means that dominance is a property worth checking.

3) *Convolution of sub-additive functions with asymptotic dominance:* We compute $\beta_{d_1, r_1, h_1} \otimes \beta_{d_2, r_2, h_2}$, where the operands are randomly generated and matching the hypotheses of Theorem 2. The impact of Theorem 2 are shown in Figure 19, which still shows speedups in the order of $10^5 \times$: unoptimized convolutions taking several minutes are often reduced to fractions of a second. However, some of the lengthy computations still take a sizable time even after the optimization. This is because the effect of Theorem 2 is to use the time of last intersection, rather than the *lcm* between the period lengths ($\text{lcm}(d_f, d_g)$), to determine the sequences to be convolved. In few cases, the former may exceed the latter, hence Theorem 2 may instead increase the cost (see the point above the bisector in the bottom-left corner of Figure 19). However, such cases are rare – and easy to avoid. In fact, we can compare the extremes of the extended domains of the operands computed with the standard algorithm and Theorem 2 and then run the algorithm that will involve fewer elementary convolutions.

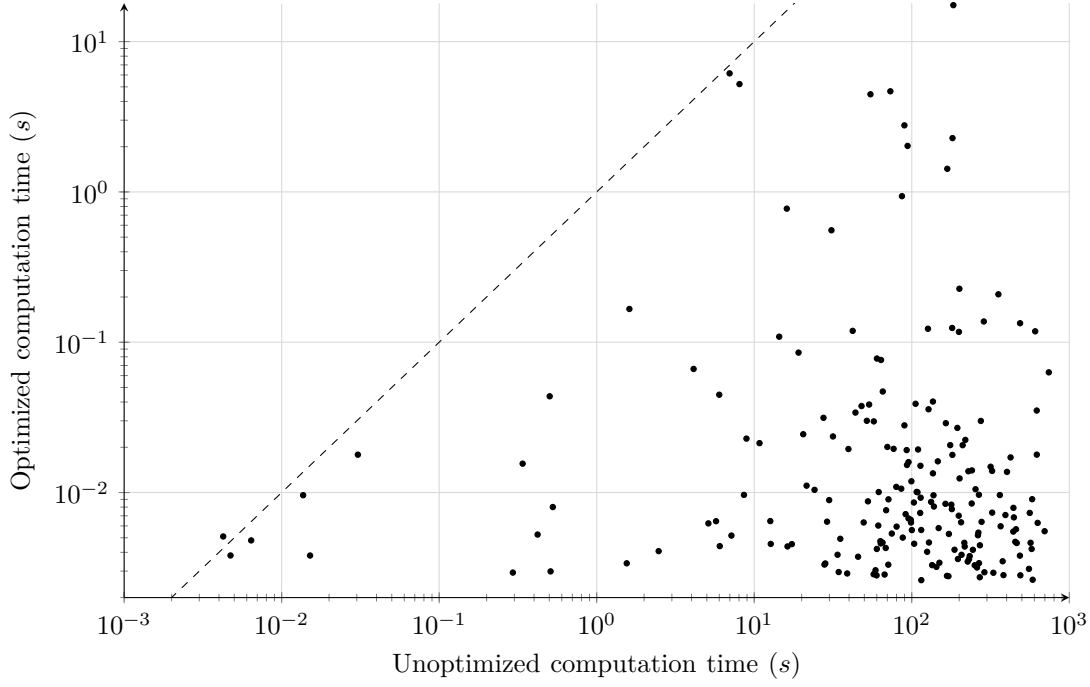


Fig. 19. Results for convolution between sub-additive functions with asymptotic dominance

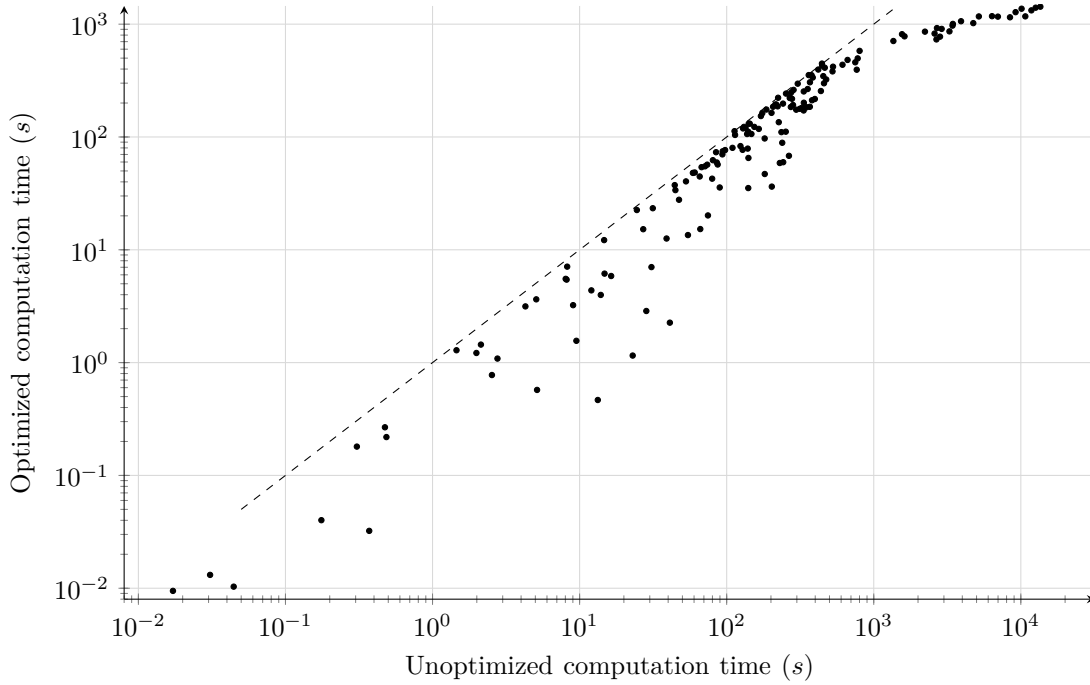


Fig. 20. Results for convolution between sub-additive functions without asymptotic dominance

4) *Convolution of sub-additive functions as self-convolution of the minimum:* A first assessment of the impact of Theorem 3 (coupled with Properties 3 and 4) is reported in Figure 20. It is evident from the figure that the speedup is less prominent in this case – the maximum that we get is 30×. Note that the higher speedups are obtained when the unoptimized computations take more time (see the top-right cluster of points). However, there is a speedup in almost all cases – we only found one outlier at 0.99×, meaning that using our theorem takes a little more time than using the basic convolution algorithm. The obtained speedup is mostly within one order of magnitude. For this reason, we report in Figure 21 a box plot of the *reduction of computation times* (which is the inverse of the speedup). With our method, computation times can be expected to be 30% to 80% of the unoptimized times.



Fig. 21. Reduction of computation times for convolution between sub-additive functions without asymptotic dominance

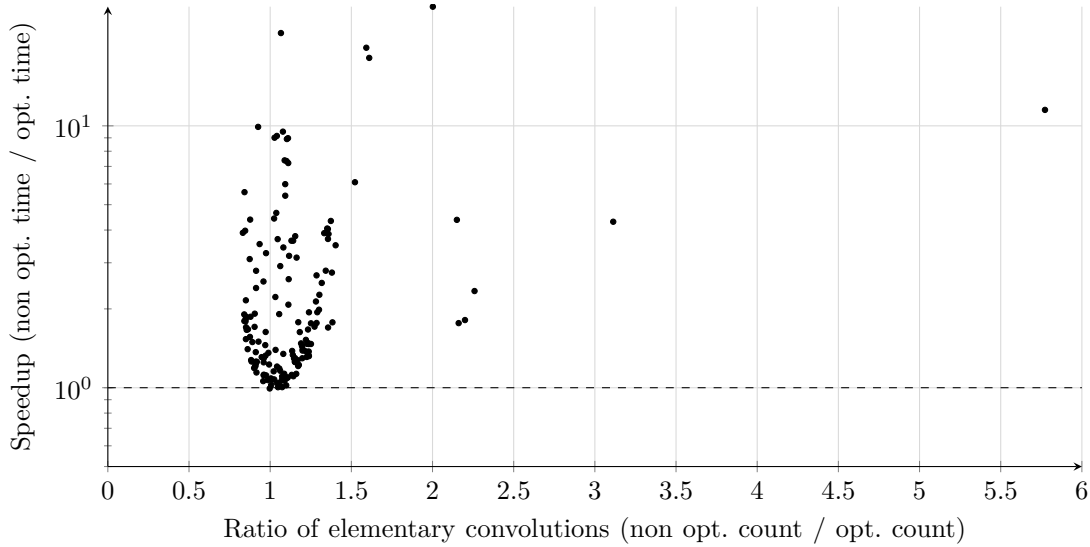


Fig. 22. Ratio of elementary convolutions vs. speedup

Intuitively, one might expect the above speedup to be related to the number of elementary convolutions. However, Figure 22 shows that this is not the case: the number of elementary convolutions is roughly the same, regardless of the achieved speedup. In more than a few cases, applying Theorem 3 entails computing *more* elementary convolutions (i.e., all the points having abscissa smaller than 1), yet the optimized version yields a nonnegligible speedup nonetheless.

The root cause of the speedups lies elsewhere. To explain it, we first need to give some details of the by-sequence convolution algorithm, namely its final step, i.e., computing the lower envelope of the elementary convolutions.

In a convolution $f \otimes g$, one must compute the elementary convolution of each element in S_f^D with each element of S_g^D (D being the extended domain, as shown in Theorem 8 in the Appendix). This yields a set E of points and segments, whose lower envelope represents the resulting sequence. The topological relationship between any two elements $x, y \in E$ is unknown a priori. They may or may not intersect, they may belong to disjoint time intervals, one may dominate the other. This is exemplified in Figure 23.

In order to compute the lower envelope of E , the first step is to determine the *intervals of overlap*, henceforth *intervals* for short. An interval I consists of a domain D_I , equal either to $[t_I, t_I]$ (point-sized) or $]t_I^s, t_I^e[$ (segment-sized), and a set

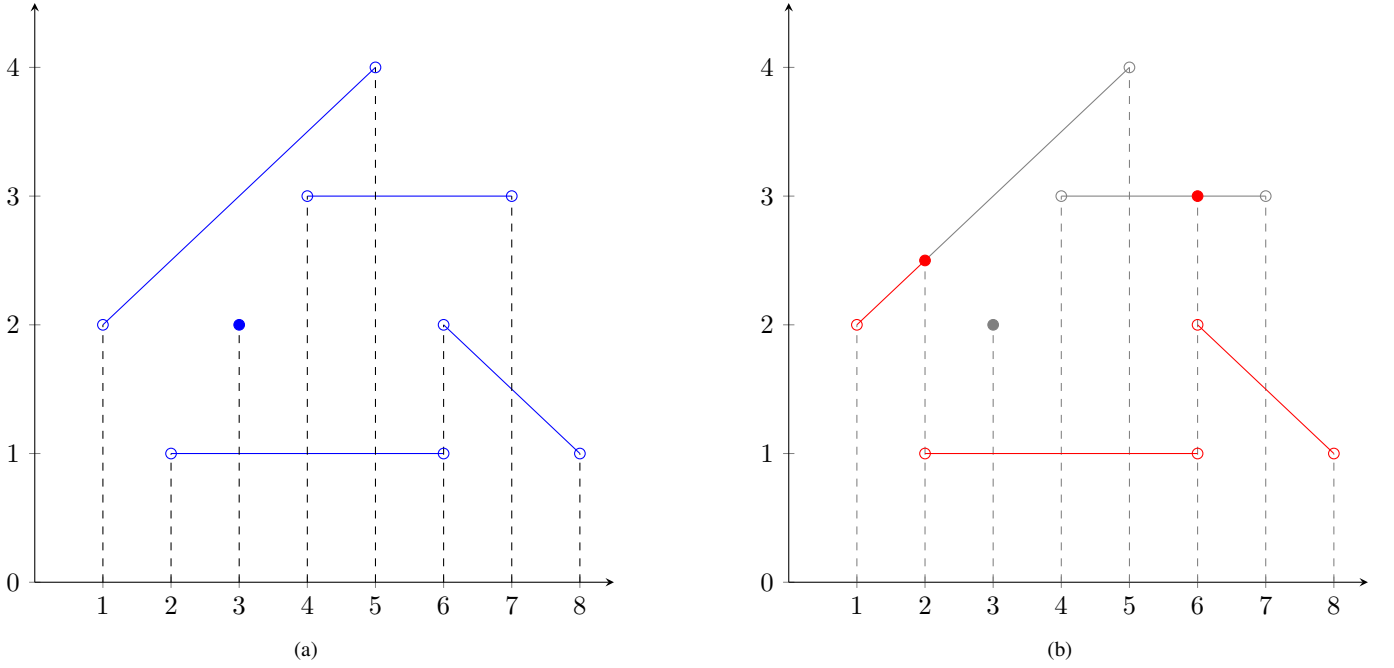


Fig. 23. Example of intervals for a set of elements (a) and their lower envelope (b)

of elements $E_I \subseteq E$ which are all the elements of E that are defined $\forall t \in D_I$. The lower envelope is computed as the juxtaposition of the lower envelopes interval by interval. To compute and populate intervals, we:

- collect the start and end times of all the elements in E and order them. Let the result be t_0, t_1, \dots, t_N ;
- derive point- and segment-sized domains for and between each of these times, i.e., $[t_0, t_0], [t_0, t_1], [t_1, t_1], \dots$;
- from the above domains, derive the set of intervals, initialized with empty lists of elements;
- for each element $e \in E$, find all the intervals e belongs to, and add e to their lists.

We underline that the element-interval relationship is many-to-many: the same element may span multiple intervals, and an interval may include several elements. Afterwards, we compute the lower envelope of each interval I , and we concatenate them to obtain the overall lower envelope of E .

As for the algorithm costs, we note that:

- 1) *finding* which intervals an element belongs to is $O(n \cdot \log(n))$, where n is the number of intervals, if one uses an interval tree;
- 2) *inserting* an element in the lists of *all the intervals* it belongs to, instead, depends on the number of intervals an element belongs to (something which we show to be highly variable in a few lines), and is $O(n)$ in a worst case;
- 3) computing the per-interval lower-envelope of I costs $O(m)$ if I is point-sized, $O(m \cdot \log(m))$ if segment-sized, where m is the cardinality of E_I ;
- 4) the concatenation of the per-interval results is $O(n)$.

Of the above steps, we note that steps 2 and 3 are independent of the number of elements, but instead depend on how much overlap there is between them. In fact, the more overlap there is between the elements of E , the higher the cost of this algorithm is. Some of the overlaps – actually, most – will not yield segments that end up being part of the lower envelope.

We show through a relevant example that computing $(f \wedge g) \otimes (f \wedge g)$ yields considerably less populated intervals than computing $f \otimes g$. The parameters are as in Table VIII.

TABLE VIII
PARAMETERS OF THE EXAMPLE CONVOLUTION

	d	r	h
f	499	901	192
g	36	806	$\frac{6912}{499}$

In the non-optimized convolution algorithm, we need to compute the lower envelope of 810k elements, for which 220k intervals are used. In the optimized algorithm, we find instead 910k elements and 320k intervals. However, as Figure 24 highlights, there is a significant difference in how many intervals each element spans. This affects the cost of step 2, which takes 180s in the non-optimized algorithm vs. 42s in the optimized one. Moreover, as Figure 25 highlights, there is also a significant difference in how many elements a given interval list includes, which affects the cost of computing the per-interval

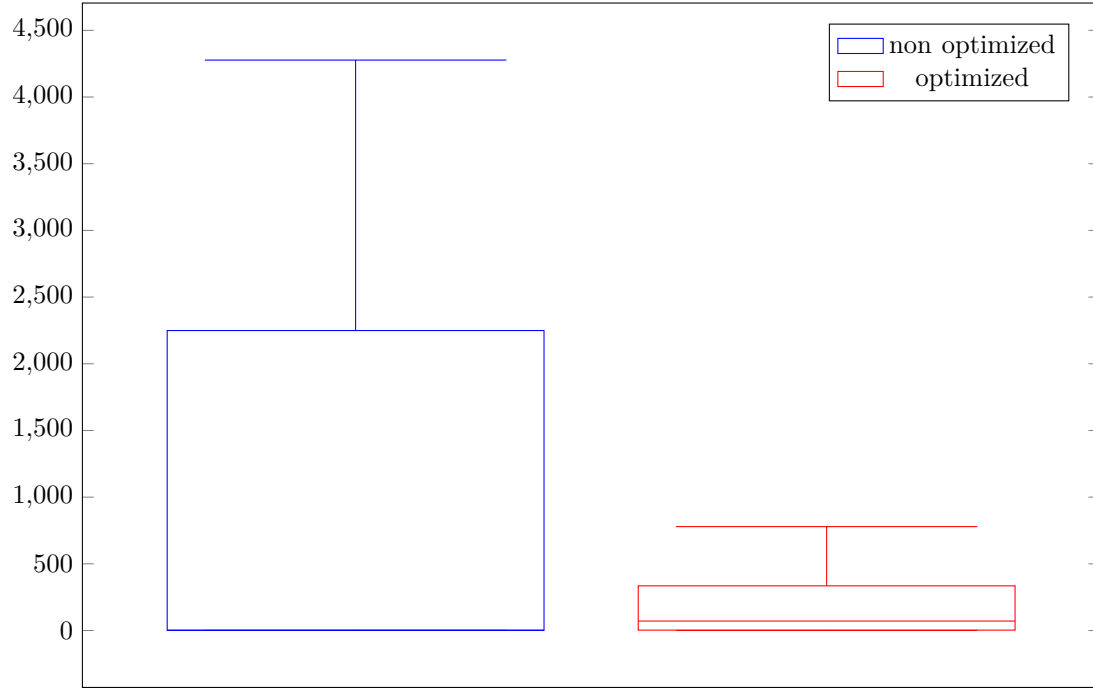


Fig. 24. Number of intervals per element

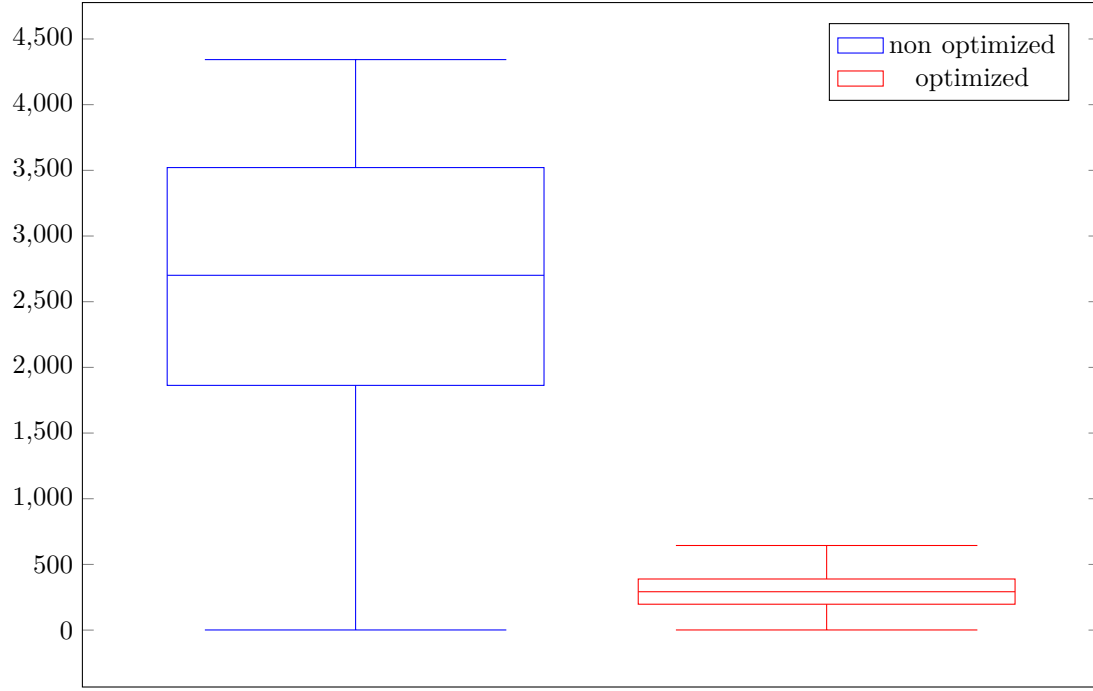


Fig. 25. Number of elements per interval

lower-envelope. In fact, step 3 takes 370s in the non-optimized algorithm, against 70s in the optimized one. Overall, applying the optimizations discussed produces, in this example, a 5× speedup – which is counter-intuitive if one considers only the number of convolutions.

B. A case study

We now show how our method allows one to analyze flow-controlled networks. We consider a tandem of n nodes, $n = 2 \dots 10$, where all nodes are described by the same rate-latency SC β , having latency $\theta = 2$ and rate $r = 16$, and with input buffers of increasing size $W = 13, 15, \dots, 29$. In Figure 26 we compare the running times of the exact method

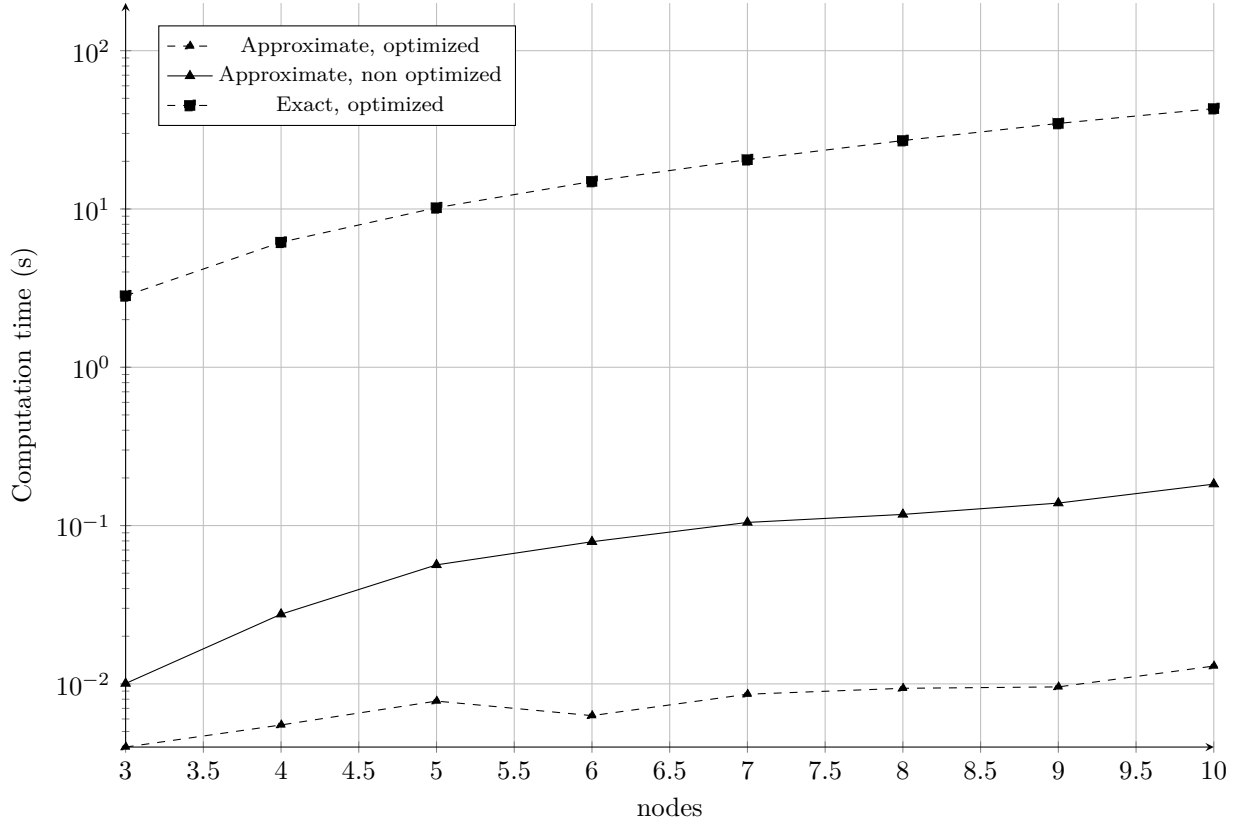


Fig. 26. Performance comparison of the exact and approximate methods

(Equation (7)) and the approximate method (Equation (9)), with and without the optimizations described in this paper. We observe that the exact method can only be run *with* our optimizations: without them, the computations for a three-node tandem had not completed after 24 hours. The graph clearly shows that the approximate method is orders of magnitude faster than even the optimized exact one. However, our optimizations still take away one order of magnitude of computations in that as well. The experiments were run five times in independent conditions, and 95% confidence intervals were always within 1% of the average. For that reason, they are not reported in the graph.

We found that the computation times (whichever the method) are very sensitive to the actual parameters of the network: changing the numbers in the above example is likely to change the vertical scale of the above graph considerably. However, the same pattern still emerges: the unoptimized exact method is just unfeasible most of the times; the optimized exact method comes second; the approximate method is considerably faster, and even faster with our optimizations.

To support the above claim, we present another scenario in Figure 27, where the computation times for the approximate method are sensibly higher. To obtain such a difference, all it took was to modify rates to $r = 1600$, latencies to $\theta = 200$, and buffer sizes to $W = 1300, 1305, \dots, 1340$. In this case, the approximate method takes up to hundreds of seconds, whereas our optimizations curb the computations at fractions of a second. It is interesting to observe that our optimization yield times that are non monotonic with the tandem length (see, e.g., around $n = 8$). This is because a more favorable optimization kicks in at $n = 8$ and further abates computation times.

What our optimizations allow – for the first time, to the best of our knowledge – is an assessment of the *accuracy* of the approximate method. In fact, this requires being able to complete exact computations, which just cannot be done without these very optimizations (unless one handpicks very trivial scenarios and parameter values, with the obvious risk of undermining generality). Our results here are quite surprising. They show that the end-to-end service curves obtained via the approximate method are *always equal* to the exact ones. This occurs not only in the tandems described in this paper, but in all the cases we analyzed, including many (several tens) with randomized configurations.

One may legitimately wonder if this is due to the fact that equality should hold in Section II-B, but so far no one was able to prove it. We show that this is not the case, i.e., there are cases when $\beta_i^{eq} > \beta_i^{eq'}$. Consider the three-node tandem in Section II-B, and assume that nodes have the same rate-latency SC β with a latency $\theta = 2$ and a rate $r = 16$, and with input buffers $W_{1,2} = 20$ and $W_{2,3} = 13$.

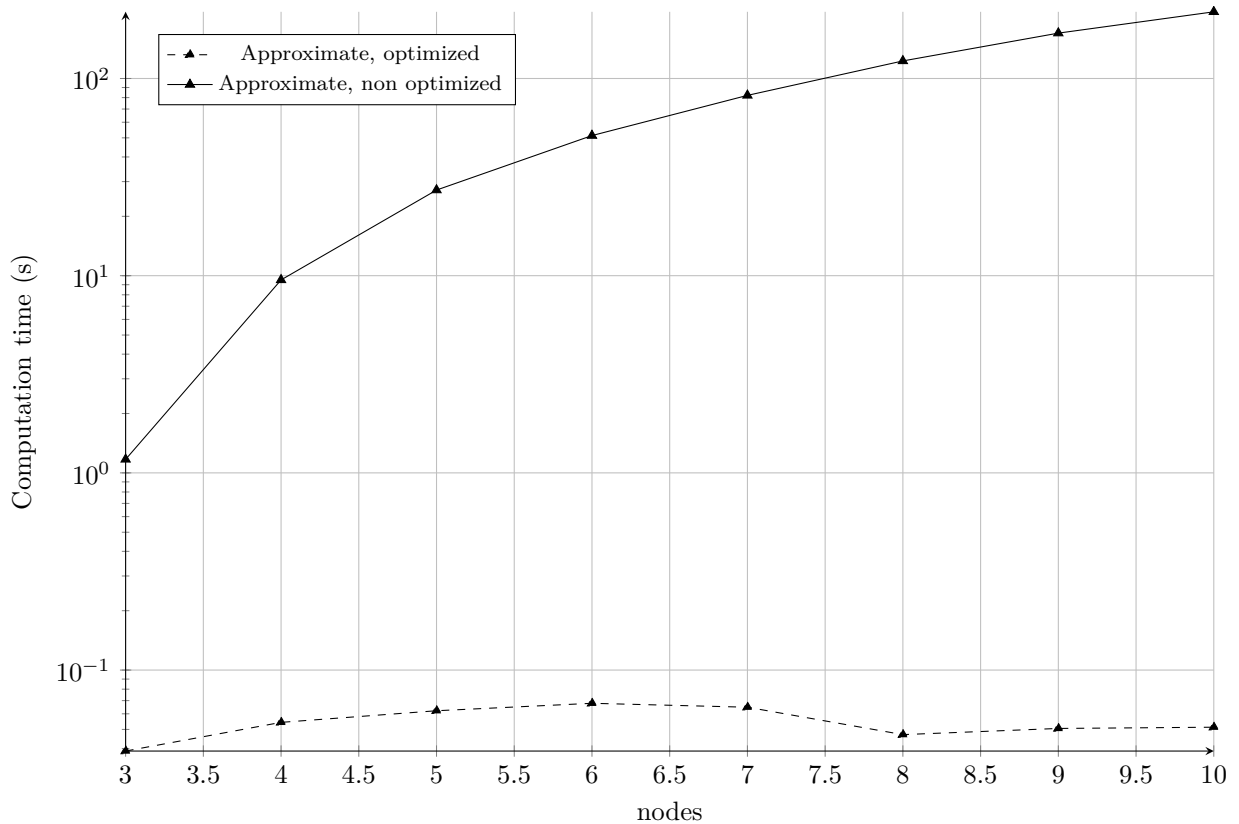


Fig. 27. Performance comparison of the approximate method

When computing the equivalent service curve at the *first* node, i.e., β_1^{eq} , $\beta_1^{eq'}$, we obtain different results using the exact and approximate method, as shown in Figure 28a. It is $\beta_1^{eq} \neq \beta_1^{eq'}$. The difference can be explained by observing that, since $W_{1,2} > W_{2,3}$, it is expected that the worst-case performance will be initially constrained by the larger buffer $W_{1,2}$ (see the first step in Figure 28a), then by the smaller buffer downstream (see the second step onwards in the same figure). The exact computation reflects this phenomenon, while the approximate method does not. However, despite this, Figure 28b shows that this difference is irrelevant when computing the equivalent service curve for the whole tandem. It is in fact $\beta^{eq} = \beta^{eq'}$. A similar phenomenon was observed in all our experiments.

The above observations cast the approximate method in a new – and more favorable light. They suggest that the latter is as performing as the exact one, in an end-to-end context. This is important, because one can always find cases where – despite our optimizations – the exact method will just be too costly.

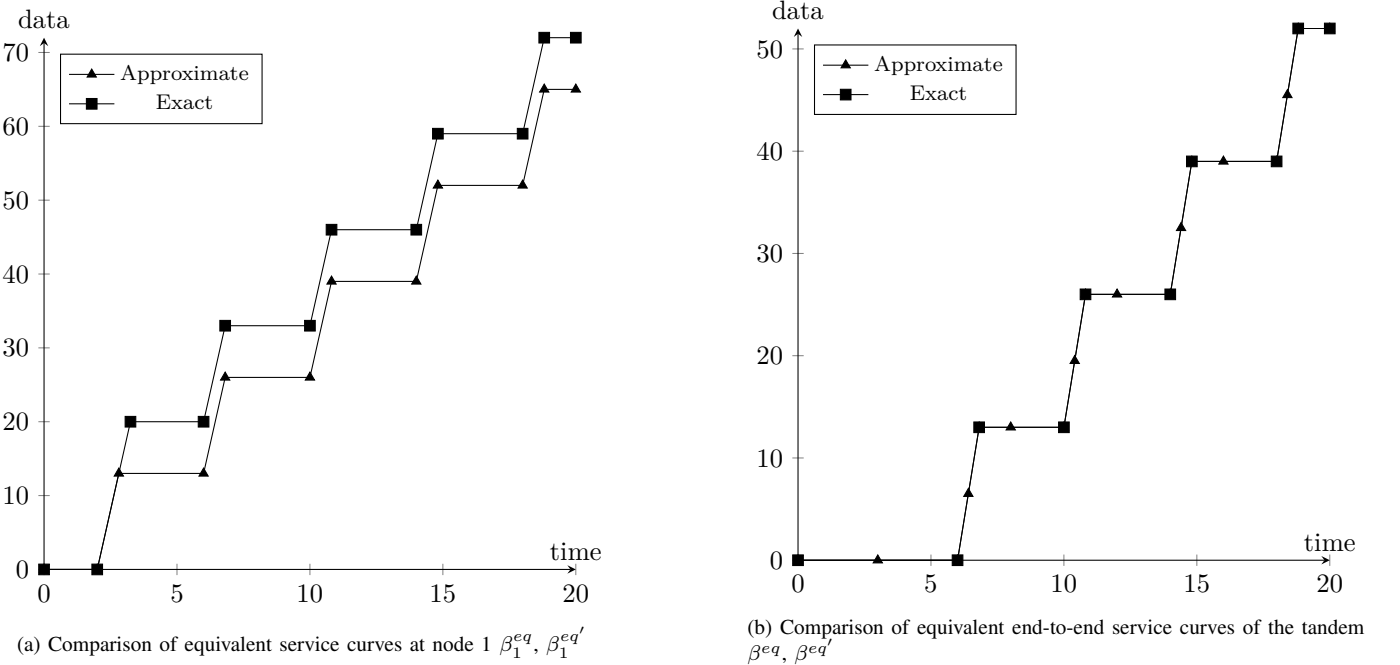


Fig. 28. Comparison of results of exact and approximate methods

VI. RELATED WORKS

The theory of Network Calculus dates back to the early 1990s, and it is mainly due to the work of Cruz [7], [8], Le Boudec and Thiran [9], and Chang [10]. Since then, a considerable number of papers have extended it to include different scheduling algorithms and flow multiplexing schemes [30]–[33], extensions to stochastic characterizations of service and traffic [34]–[36], specific network architectures [4], [5], [27], [37]–[39].

The *computational* aspects of NC implementations have been the subject of several papers in the past. Problems such as efficient data structures to represent arrival/service curves or functions, or the complexity of NC operators (e.g., convolution or sub-additive closure) have been tackled in the works of Bouillard et al. [25], and find a thorough exposition in book [26], which also reviews the implementations of several existing tools. The idea of UPP curves as a class closed with respect to NC operations is in fact reported in these works. We use the NC algorithms described therein as a baseline. A related research field is that of Real-time Calculus (RTC), developed for real-time systems [40]. RTC is based on min-plus and max-plus operators that work on Variability Characterization Curves, which appear to be very similar to UPP functions (although work [25] observes that the two classes treat discontinuities in a different way, and [41] remarks that they were never formally compared). RTC uses min-plus convolution to obtain the output of a system given its input, similarly to NC. For this reason, the two methodologies have often evolved via cross-fertilization, with solutions devised in one context often being ported to the other. In fact, RTC work [28] first observed that multi-hop traversal – which entails chained convolutions – is subject to representation explosion, and that the latter makes convolutions exponentially complex. They propose a way to mitigate this problem, which relies on inferring the maximum time beyond which the shape of the resulting functions is immaterial, which turns out to be considerably smaller than the *lcm* of the periods, thus leading to more efficient operations. This idea of a compact domain is transferred to NC in [29] – allowing it to be used in conjunction with NC service curves. Work [42] further generalizes it to more operations and more general RTC settings. NC analysis limited to compact domains [29] consists in finding finite upper bounds to the time where operations should be computed. This allows by-sequence operations to be computed between two finite sets of elements – which one can imagine as transient parts – disregarding periodicity and the *lcm* explosion that comes with it. The upper bound is chosen so that the end-to-end delay and backlog analysis is not affected. This is done by working with lower/upper CPL approximations of *both* the arrival curve and the service curves, which is computationally inexpensive. As already explained, this method cannot be applied to our problem, since it leverages *super-additivity* of service curves, a property that does not hold in our settings.

As far as NC *tools* are concerned, a critical review of the available software packages is reported in [43]. However, the latter only reports *functional* comparisons (i.e., discusses the capabilities of each tool), and does not address performance issues. To the best of our knowledge, there seems to be no *open* NC tool that is able to deal with UPP functions. Most of the existing public tools, e.g., CyNC [44], NC-Maude [45], DiscoDNC [46], DEBORAH [47], [48], CATS [49] restrict the implementation of NC operators to the case of convex or concave piecewise-linear functions (CPL). This means that they cannot be used to run the computations described in this paper. The COINC library [50] did address UPP (implementing the algorithms in [25]), but

it appears that it is no longer available. Commercial tool Real-Time-at-Work (RTaW) can perform min-plus computations on UPP functions, and is also available via a browser-based interpreter [51]. However, its license explicitly prohibits using it for benchmarking purposes. The RTC algorithmic toolbox [52] is a Java-based tool for RTC analysis, available also as a Matlab toolbox, which implements a general-purpose convolution operator, that should be able to run – in theory – the examples of Section V. To the best of our knowledge, RTC’s source code is not available at the time of writing this paper. We have no indication that it uses our findings in its computations. However, RTC uses floating-point arithmetics, which means that it may be subject to numerical errors whose impact is difficult to assess. Our arithmetics is based instead on rational numbers, hence computations are always exact. Moreover, it seems that RTC loops infinitely in several cases – which are not challenging, performance-wise.

Systems with flow control have traditionally been analyzed using Markov Chains [6], under the name of "queueing systems with blocking". That method allows one to find mean performance indexes (and, possibly, distributions), starting from a *stochastic* characterization of input traffic and service. The first works analyzing flow control in the framework of NC have been [53], [54]. The exact method – i.e., the one using nested SACs – is a direct application of these results. The approximate method – i.e., the one using convolution of SACs – is instead shown in [27]. This paper, however, does not assess the gain in efficiency warranted by the approximate method, nor it acknowledges the fact that it seems to preserve accuracy. We argue that this may be due to the fact that the computational problems addressed in this paper were in the way of such an evaluation. Paper [55] uses a NC model with flow control to model Denial-of-Service (DOS) attacks. Flow control is also addressed in [56], in the framework of *stochastic* NC.

VII. CONCLUSIONS AND FUTURE WORK

In this paper, we addressed the problem of analyzing tandems of flow-controlled network elements. We reviewed the available methods, both exact and approximated, and highlighted that both can be onerous from a computation standpoint. The exact method, in particular, scales rather poorly with the tandem length, virtually making analysis infeasible if the tandem has three or more hops. We showed that the approximate method – although more affordable – may still scale poorly. We traced back the problem to the explosion of periods in the convolution of ultimately pseudo-periodic curves, a problem which cannot be mitigated using known techniques (which rely on hypotheses that our service curves fail to verify). We then presented novel computational and algebraic techniques to reduce the computation time of convolutions. Our first technique consists in minimizing the representation of a function after every operation. In fact, the existing algorithms for NC operations yield non-minimal representations, and the length of a representation is the dominating factor in the complexity of the algorithms. We showed that minimization is computationally cheap. It may yield reductions in the representation size of orders of magnitude. This translates to a similar reduction in the *number* of elementary convolutions involved in a SAC, hence acting an enabler for exact analysis. Moreover, by reducing the length of the periods, it may also reduce the *lcm* of the periods of the operands in a convolution, thus making it more efficient. On top of that, we presented novel algebraic properties of sub-additive functions that lead to optimized convolution algorithms. More specifically, we showed that the convolution of sub-additive functions with *different rates* can be greatly simplified: it boils down to a simple minimum if one dominates the other, and it is greatly simplified otherwise. Our computational results show that these convolutions can be made quite simple.

Moreover, when two functions have the same rate and intersect an infinite number of times, we can transform their convolution into a self-convolution of their minimum. Self-convolution of a minimum is a rather efficient operation, since – on one hand – it allows one to filter away several elementary convolutions, thus reducing the computation time, and – on the other – it yields sequence elements that have better topological properties, making the final computation of a lower envelope considerably more efficient. We have showed that the speedup brought by our algebraic properties ranges from two-digit percentages (especially in the case of infinitely intersecting functions with the same rate) to several orders of magnitude (in the other cases), even factoring in the time required to check the properties themselves. The cases when little or nothing is gained in the way of efficiency are a small minority, and can often be identified *a priori*. Our optimizations allowed us to compare the exact and approximate analysis methods, as for efficiency and accuracy, something that could not be done before due to the prohibitive times involved in the computations. Our results are that – rather surprisingly – the approximate method seems to be as accurate as the exact one, because differences in the per-node equivalent service curves get erased in an end-to-end context. This is particularly important, since the approximate method scales considerably better than the exact one.

We observe that the techniques outlined in this paper may lend themselves to other applications. For instance, representation minimization can always be applied when performing NC operations on UPP curves. Sub-additive UPP curves, moreover, may come up for other reasons than the curve being the result of a SAC.

There are several directions in which our work can be expanded. On the algebraic side, looking for other classes of functions (beside sub-additive ones) for which similar properties as those shown in this paper hold, possibly leading to similar simplifications. Moreover, the fact that – in all the experiments we performed – the exact and approximate method end up computing the same end-to-end service curve from different per-node service curves, clearly calls for further investigation. On the computational side, we can observe that several of the complex tasks to be performed with operations (e.g., finding the lower envelope interval by interval) are amenable to parallel implementation. Our NC library already supports parallelization,

thus our next endeavor is to investigate this avenue further, to understand what can be gained by distributing what tasks among parallel threads.

VIII. ACKNOWLEDGEMENTS

This work was supported in part by the Italian Ministry of Education and Research (MIUR) in the framework of the CrossLab project (Departments of Excellence), and by the University of Pisa, through grant “Analisi di reti complesse: dalla teoria alle applicazioni” - PRA 2020.

REFERENCES

- [1] P. Goyal, P. Shah, N. K. Sharma, M. Alizadeh and T. E. Anderson, “Backpressure flow control,” in *Proceedings of the 2019 Workshop on Buffer Sizing*, ser. BS ’19, Palo Alto, CA, USA: Association for Computing Machinery, 2019, ISBN: 9781450377454. DOI: 10.1145/3375235.3375239. [Online]. Available: <https://doi.org/10.1145/3375235.3375239>.
- [2] S.-Y. Wang, Y.-R. Chen, H.-C. Hsieh, R.-S. Lai and Y.-B. Lin, “A flow control scheme based on per hop and per flow in commodity switches for lossless networks,” *IEEE Access*, vol. 9, pp. 156 013–156 029, 2021. DOI: 10.1109/ACCESS.2021.3129595.
- [3] L. Guo and P. Congdon, “Ieee 802 nendica report: Intelligent lossless data center networks,” *IEEE SA Industry Connections–IEEE 802 Nendica Report: Intelligent Lossless Data Center Networks*, pp. 1–44, 2021.
- [4] Y. Qian, Z. Lu and W. Dou, “Analysis of worst-case delay bounds for best-effort communication in wormhole networks on chip,” in *Networks-on-Chip, 2009. NoCS 2009. 3rd ACM/IEEE International Symposium on*, IEEE, 2009, pp. 44–53.
- [5] —, “Analysis of worst-case delay bounds for on-chip packet-switching networks,” *IEEE Transactions on Computer-Aided Design of Integrated Circuits and Systems*, vol. 29, no. 5, pp. 802–815, 2010.
- [6] S. Balsamo, “Queueing networks with blocking: Analysis, solution algorithms and properties,” in *Network Performance Engineering: A Handbook on Convergent Multi-Service Networks and Next Generation Internet*, D. D. Kouvatsos, Ed. Berlin, Heidelberg: Springer Berlin Heidelberg, 2011, pp. 233–257, ISBN: 978-3-642-02742-0. DOI: 10.1007/978-3-642-02742-0_11. [Online]. Available: https://doi.org/10.1007/978-3-642-02742-0_11.
- [7] R. L. Cruz *et al.*, “A calculus for network delay, part I: Network elements in isolation,” *IEEE Transactions on information theory*, vol. 37, no. 1, pp. 114–131, 1991.
- [8] R. L. Cruz, “A calculus for network delay, part II: Network analysis,” *IEEE Transactions on information theory*, vol. 37, no. 1, pp. 132–141, 1991.
- [9] J.-Y. Le Boudec and P. Thiran, *Network calculus: a theory of deterministic queueing systems for the internet*. Springer Science & Business Media, 2001, vol. 2050.
- [10] C.-S. Chang, *Performance guarantees in communication networks*. Springer-Verlang, 2000.
- [11] J.-Y. Le Boudec, “Application of network calculus to guaranteed service networks,” *IEEE Transactions on Information theory*, vol. 44, no. 3, pp. 1087–1096, 1998.
- [12] V. Firoiu, J.-Y. Le Boudec, D. Towsley and Z.-L. Zhang, “Theories and models for internet quality of service,” *Proceedings of the IEEE*, vol. 90, no. 9, pp. 1565–1591, 2002.
- [13] J.-Y. Le Boudec, “Application of network calculus to guaranteed service networks,” *IEEE Transactions on Information Theory*, vol. 44, no. 3, pp. 1087–1096, 1998. DOI: 10.1109/18.669170.
- [14] J. C. Bennett, K. Benson, A. Charny, W. F. Courtney and J.-Y. Le Boudec, “Delay jitter bounds and packet scale rate guarantee for expedited forwarding,” *IEEE/ACM Transactions on networking*, vol. 10, no. 4, pp. 529–540, 2002.
- [15] M. Fidler and V. Sander, “A parameter based admission control for differentiated services networks,” *Computer Networks*, vol. 44, no. 4, pp. 463–479, 2004.
- [16] J. B. Schmitt and U. Roedig, “Sensor network calculus—a framework for worst case analysis,” in *International Conference on Distributed Computing in Sensor Systems*, Springer, 2005, pp. 141–154.
- [17] H. Charara, J.-L. Scharbarg, J. Ermont and C. Fraboul, “Methods for bounding end-to-end delays on an afdx network,” in *18th Euromicro Conference on Real-Time Systems (ECRTS’06)*, IEEE, 2006, 10–pp.
- [18] H. Bauer, J.-L. Scharbarg and C. Fraboul, “Worst-case end-to-end delay analysis of an avionics afdx network,” in *2010 Design, Automation & Test in Europe Conference & Exhibition (DATE 2010)*, IEEE, 2010, pp. 1220–1224.
- [19] J. Zhang, L. Chen, T. Wang and X. Wang, “Analysis of tsn for industrial automation based on network calculus,” in *2019 24th IEEE International Conference on Emerging Technologies and Factory Automation (ETFA)*, IEEE, 2019, pp. 240–247.
- [20] L. Maile, K.-S. Hielscher and R. German, “Network calculus results for tsn: An introduction,” in *2020 Information Communication Technologies Conference (ICTC)*, IEEE, 2020, pp. 131–140.
- [21] L. Zhao, P. Pop, Z. Zheng, H. Daigmorte and M. Boyer, “Latency analysis of multiple classes of AVB traffic in TSN with standard credit behavior using network calculus,” *IEEE Trans. Ind. Electron.*, vol. 68, no. 10, pp. 10 291–10 302, 2021. DOI: 10.1109/TIE.2020.3021638. [Online]. Available: <https://doi.org/10.1109/TIE.2020.3021638>.

[22] F. Rehm, J. Seitter, J.-P. Larsson, S. Saidi, G. Stea, R. Zippo, D. Ziegenbein, M. Andreozzi and A. Hamann, “The road towards predictable automotive high-performance platforms,” in *2021 Design, Automation & Test in Europe Conference & Exhibition (DATE)*, IEEE, 2021, pp. 1915–1924.

[23] M. Andreozzi, F. Conboy, G. Stea and R. Zippo, “Heterogeneous systems modelling with adaptive traffic profiles and its application to worst-case analysis of a dram controller,” in *2020 IEEE 44th Annual Computers, Software, and Applications Conference (COMPSAC)*, IEEE, 2020, pp. 79–86.

[24] M. Boyer, A. Graillat, B. D. de Dinechin and J. Migge, “Bounding the delays of the MPPA network-on-chip with network calculus:models and benchmarks,” *Perform. Evaluation*, vol. 143, p. 102 124, 2020. DOI: 10.1016/j.peva.2020.102124. [Online]. Available: <https://doi.org/10.1016/j.peva.2020.102124>.

[25] A. Bouillard and E. Thierry, “An Algorithmic Toolbox for Network Calculus,” INRIA, Research Report RR-6094, 2007, p. 44. [Online]. Available: <https://hal.inria.fr/inria-00123643>.

[26] A. Bouillard, M. Boyer and E. Le Corronc, *Deterministic Network Calculus: From Theory to Practical Implementation*. Wiley, 2018.

[27] A. Bose, X. Jiang, B. Liu and G. Li, “Analysis of manufacturing blocking systems with network calculus,” *Performance Evaluation*, vol. 63, no. 12, pp. 1216–1234, 2006.

[28] N. Guan and W. Yi, “Finitary real-time calculus: Efficient performance analysis of distributed embedded systems,” in *2013 IEEE 34th Real-Time Systems Symposium*, 2013, pp. 330–339. DOI: 10.1109/RTSS.2013.40.

[29] K. Lampka, S. Bondorf and J. Schmitt, “Achieving efficiency without sacrificing model accuracy: Network calculus on compact domains,” in *2016 IEEE 24th International Symposium on Modeling, Analysis and Simulation of Computer and Telecommunication Systems (MASCOTS)*, IEEE, 2016, pp. 313–318.

[30] L. Lenzini, L. Martorini, E. Mingozi and G. Stea, “Tight end-to-end per-flow delay bounds in FIFO multiplexing sink-tree networks,” *Performance Evaluation*, vol. 63, no. 9-10, pp. 956–987, 2006.

[31] A. Bouillard and G. Stea, “Exact worst-case delay in FIFO-multiplexing feed-forward networks,” *IEEE/ACM Transactions on Networking (TON)*, vol. 23, no. 5, pp. 1387–1400, 2015.

[32] S. M. Tabatabaei and J.-Y. L. Boudec, “Deficit round-robin: A second network calculus analysis,” in *2021 IEEE 27th Real-Time and Embedded Technology and Applications Symposium (RTAS)*, 2021, pp. 171–183. DOI: 10.1109/RTAS52030.2021.00022.

[33] A. Bouillard, “Individual service curves for bandwidth-sharing policies using network calculus,” *IEEE Networking Letters*, vol. 3, no. 2, pp. 80–83, 2021. DOI: 10.1109/LNET.2021.3067766.

[34] Y. Jiang, “A basic stochastic network calculus,” in *Proceedings of the 2006 Conference on Applications, Technologies, Architectures, and Protocols for Computer Communications*, ser. SIGCOMM ’06, Pisa, Italy: Association for Computing Machinery, 2006, pp. 123–134, ISBN: 1595933085. DOI: 10.1145/1159913.1159929. [Online]. Available: <https://doi.org/10.1145/1159913.1159929>.

[35] M. Fidler, “Survey of deterministic and stochastic service curve models in the network calculus,” *IEEE Communications Surveys Tutorials*, vol. 12, no. 1, pp. 59–86, 2010. DOI: 10.1109/SURV.2010.020110.00019.

[36] M. Fidler and A. Rizk, “A guide to the stochastic network calculus,” *IEEE Communications Surveys Tutorials*, vol. 17, no. 1, pp. 92–105, 2015. DOI: 10.1109/COMST.2014.2337060.

[37] J. B. Schmitt and U. Roedig, “Sensor network calculus – a framework for worst case analysis,” in *Distributed Computing in Sensor Systems*, V. K. Prasanna, S. S. Iyengar, P. G. Spirakis and M. Welsh, Eds., Berlin, Heidelberg: Springer Berlin Heidelberg, 2005, pp. 141–154, ISBN: 978-3-540-31671-8.

[38] A. Soni, X. Li, J.-L. Scharbarg and C. Fraboul, “Optimizing network calculus for switched ethernet network with deficit round robin,” in *2018 IEEE Real-Time Systems Symposium (RTSS)*, 2018, pp. 300–311. DOI: 10.1109/RTSS.2018.00046.

[39] L. Maile, K.-S. Hielscher and R. German, “Network calculus results for tsn: An introduction,” in *2020 Information Communication Technologies Conference (ICTC)*, 2020, pp. 131–140. DOI: 10.1109/ICTC49638.2020.9123308.

[40] L. Thiele, S. Chakraborty and M. Naedele, “Real-time calculus for scheduling hard real-time systems,” in *2000 IEEE International Symposium on Circuits and Systems (ISCAS)*, IEEE, vol. 4, 2000, pp. 101–104.

[41] L. Rakotomalala, P. Roux and M. Boyer, “Verifying min-plus computations with coq,” in *NASA Formal Methods*, A. Dutle, M. M. Moscato, L. Titolo, C. A. Muñoz and I. Perez, Eds., Cham: Springer International Publishing, 2021, pp. 287–303, ISBN: 978-3-030-76384-8.

[42] K. Lampka, S. Bondorf, J. B. Schmitt, N. Guan and W. Yi, “Generalized finitary real-time calculus,” in *IEEE INFOCOM 2017 - IEEE Conference on Computer Communications*, 2017, pp. 1–9. DOI: 10.1109/INFOCOM.2017.8056981.

[43] B. Zhou, I. Howenstine, S. Limprapaipong and L. Cheng, “A survey on network calculus tools for network infrastructure in real-time systems,” *IEEE Access*, vol. 8, pp. 223 588–223 605, 2020. DOI: 10.1109/ACCESS.2020.3043600.

[44] H. Schioeler, H.-P. Schwefel and M. B. Hansen, “Cync: A matlab/simulink toolbox for network calculus.,” in *ValueTools*, Citeseer, 2007, p. 60.

[45] M. Boyer, “Nc-maude: A rewriting tool to play with network calculus,” in *Leveraging Applications of Formal Methods, Verification, and Validation - 4th International Symposium on Leveraging Applications, ISoLA 2010, Heraklion, Crete, Greece, October 18-21, 2010, Proceedings, Part I*, T. Margaria and B. Steffen, Eds., ser. Lecture Notes in Computer

Science, vol. 6415, Springer, 2010, pp. 137–151. DOI: 10.1007/978-3-642-16558-0\14. [Online]. Available: https://doi.org/10.1007/978-3-642-16558-0%5C_14.

[46] S. Bondorf and J. B. Schmitt, “The DiscodNC v2: A Comprehensive Tool for Deterministic Network Calculus,” in *Proceedings of the 8th International Conference on Performance Evaluation Methodologies and Tools*, ser. VALUETOOLS ’14, Bratislava, Slovakia: ICST (Institute for Computer Sciences, Social-Informatics and Telecommunications Engineering), 2014, pp. 44–49, ISBN: 9781631900570. DOI: 10.4108/icst.Valuetools.2014.258167. [Online]. Available: <https://doi.org/10.4108/icst.Valuetools.2014.258167>.

[47] L. Bisti, L. Lenzini, E. Mingozi and G. Stea, “Deborah: A tool for worst-case analysis of FIFO tandems,” in *International Symposium On Leveraging Applications of Formal Methods, Verification and Validation*, Springer, 2010, pp. 152–168.

[48] ———, “Numerical analysis of worst-case end-to-end delay bounds in FIFO tandem networks,” *Real-Time Systems*, vol. 48, no. 5, pp. 527–569, 2012.

[49] P. Krcál, L. Mokrushin and W. Yi, “A tool for compositional analysis of timed systems by abstraction,” in *Proceedings of 19th Nordic workshop on programming theory (NWPT07)*, 2007.

[50] A. Bouillard, B. Cottenceau, B. Gaujal, L. Hardouin, S. Lagrange and M. Lhommeau, “Coinc library: A toolbox for the network calculus: Invited presentation, extended abstract,” in *Proceedings of the Fourth International ICST Conference on Performance Evaluation Methodologies and Tools*, ser. VALUETOOLS ’09, Pisa, Italy: ICST (Institute for Computer Sciences, Social-Informatics and Telecommunications Engineering), 2009, ISBN: 9789639799707.

[51] RealTime-at-Work, *Online min-plus interpreter for network calculus*, <http://realtimeatwork.com/minplus-playground>. (visited on 01/11/2021).

[52] E. Wandeler and L. Thiele, *Real-Time Calculus (RTC) Toolbox*, <http://www.mpa.ethz.ch/Rtctoolbox>. [Online]. Available: <http://www.mpa.ethz.ch/Rtctoolbox> (visited on 01/11/2021).

[53] C.-s. Chang, “On deterministic traffic regulation and service guarantees: A systematic approach by filtering,” *IEEE Transactions on Information Theory*, vol. 44, pp. 1096–1107, 1997.

[54] R. Agrawal, R. L. Cruz, C. Okino and R. Rajan, “Performance bounds for flow control protocols,” *IEEE/ACM Transactions on Networking*, vol. 7, pp. 310–323, 1998.

[55] V. G. Promyslov and K. V. Semenkov, “Assessment of deterministic delay bounds for a dos-attack prevention device with a static window flow control,” *IFAC-PapersOnLine*, vol. 53, no. 2, pp. 11 089–11 093, 2020, 21st IFAC World Congress, ISSN: 2405-8963. DOI: <https://doi.org/10.1016/j.ifacol.2020.12.251>. [Online]. Available: <https://www.sciencedirect.com/science/article/pii/S2405896320305280>.

[56] M. Beck and J. Schmitt, “Generalizing window flow control in bivariate network calculus to enable leftover service in the loop,” *Performance Evaluation*, vol. 114, pp. 45–55, 2017, ISSN: 0166-5316. DOI: <https://doi.org/10.1016/j.peva.2017.04.008>. [Online]. Available: <https://www.sciencedirect.com/science/article/pii/S0166531616301808>.

APPENDIX

We report below the proofs of the algorithms to compute the results of min-plus operations for ultimately pseudo-periodic piecewise affine $\mathbb{Q}_+ \rightarrow \mathbb{Q}$ functions. Proofs are adapted from those in [25], with a few clarifications of our own. The *stability* of min-plus operators for the above class of functions is discussed in [25]. For the sake of conciseness, we will not discuss here how to compute elementary operations, i.e., between points, segments and limited piecewise sequences.

We recall that, for ultimately pseudo-periodic piecewise affine $\mathbb{Q}_+ \rightarrow \mathbb{Q}$ functions,

- $f(t + k \cdot d) = f(t) + k \cdot c \ \forall t \geq T, k \in \mathbb{N}$
- $\rho = c/d$

MINIMUM

For the minimum $f_1 \wedge f_2$, we need to treat the following two cases separately:

- $\rho_1 = \rho_2$
- $\rho_1 < \rho_2$ (without loss of generality, minimum being commutative)

Theorem 4 (Minimum of pseudo-periodic functions with the same rate). *If $\rho_1 = \rho_2$ (say ρ), $\min(f_1, f_2)$ is pseudo-periodic for $T = \max(T_1, T_2)$, $d = \text{lcm}(d_1, d_2)$, $c = \rho \cdot d$*

Proof.

$$\begin{aligned} \forall t \geq \max(T_1, T_2) \\ (\min(f_1, f_2))(t + d) &= \min(f_1(t + d), f_2(t + d)) \\ &= \min(f_1(t) + \frac{d}{d_1} \cdot c_1, f_2(t) + \frac{d}{d_2} \cdot c_2) \\ &= \min(f_1(t) + \rho \cdot d, f_2(t) + \rho \cdot d) \\ &= \min(f_1(t), f_2(t)) + \rho \cdot d \end{aligned}$$

We observe that, in order to be able to leverage the pseudo-periodicity property to both f_1 and f_2 in this proof:

- It is enough that t is above both T_1 and T_2 independently, i.e., $t = \max(T_1, T_2)$
- It is necessary that $d = \text{lcm}(d_1, d_2)$, as both $\frac{d}{d_1}$ and $\frac{d}{d_2}$ need to be $\in \mathbb{N}$

□

Theorem 5 (Minimum of pseudo-periodic functions with different rates). *If $\rho_1 < \rho_2$, $\exists \bar{t} : \forall t \geq \bar{t}, f_1(t) \leq f_2(t)$. In particular, we can compute \bar{t} as follows:*

- Define the upper boundary of the pseudo-periodic behavior of f_1 as the line $U_1(t)$ such that $f_1(t) \leq U_1(t) \ \forall t \geq T_1$. We can compute this as $U_1(t) = \rho_1 \cdot t + M_1$ where $M_1 = \sup_{T_1 \leq t < T_1 + d_1} (f_1(t) - \rho_1 \cdot t)$
- Define the lower boundary of the pseudo-periodic behavior of f_2 as the line $l_2(t)$ such that $f_2(t) \geq l_2(t) \ \forall t \geq T_2$. We can compute this as $l_2(t) = \rho_2 \cdot t + m_2$ where $m_2 = \inf_{T_2 \leq t < T_2 + d_2} (f_2(t) - \rho_2 \cdot t)$
- Then we can bound \bar{t} through $U_1(\bar{t}) \leq l_2(\bar{t})$, i.e., $\bar{t} \geq \frac{M_1 - m_2}{\rho_2 - \rho_1}$. Note that, by construction, this bound is valid only if $\bar{t} \geq \max(T_1, T_2)$.

Then $\min(f_1, f_2)$ is pseudo-periodic for $T = \max(T_1, T_2, \bar{t})$, $d = d_1$, $c = c_1$

Proof.

We distinguish two cases, i.e., when the last intersection between f_1 and f_2 occurs before or after the start of their pseudo-periodic behaviors.

If before, it is enough to consider $T = \max(T_1, T_2)$ to have all the information for $\min(f_1, f_2)$. Otherwise, we can use the bound $\bar{t} \geq \max(T_1, T_2)$ as T for the same purpose.

Both cases are represented by the expression $T = \max(T_1, T_2, \bar{t})$, which guarantees that $\min(f_1, f_2)(t) = f_1(t) \ \forall t \geq T$. Then:

$$\begin{aligned} \forall t \geq \max(T_1, T_2, \bar{t}) \\ (\min(f_1, f_2))(t + d_1) &= \min(f_1(t + d_1), f_2(t + d_1)) \\ &= f_1(t + d_1) \\ &= f_1(t) + c_1 \\ &= \min(f_1(t), f_2(t)) + c_1 \end{aligned}$$

□

CONVOLUTION

First, we decompose both functions, f and g , in their transient and periodic parts: $f = \min(f_t, f_p)$, where

- $f_t(t) = f(t) \forall t \in [0, T_f[; f_t(t) = +\infty \text{ otherwise}$
- $f_p(t) = f(t) \forall t \in [T_f, +\infty[; f_p(t) = +\infty \text{ otherwise}$

Then, we can decompose the convolution as:

$$\begin{aligned} f \otimes g &= \min(f_t, f_p) \otimes \min(g_t, g_p) \\ &= \min(f_t \otimes g_t, f_t \otimes g_p, f_p \otimes g_t, f_p \otimes g_p) \end{aligned}$$

We discuss first how the above partial convolutions are computed, and then what are the properties of the final result.

For the first term, we observe that $f_t \otimes g_t$ is defined in $[0, T_f + T_g[$ and is equal to $+\infty$ for $t \geq T_f + T_g$.

For the second and third terms, we have the following result:

Theorem 6 (Convolution of transient and periodic part). $f_t \otimes g_p$ is pseudo-periodic from $T_f + T_g$ with period d_g and increment c_g . The symmetric result holds for $f_p \otimes g_t$.

Proof. Since $f_t(t) = +\infty$ for all $t \geq T_f$, we can write – for all $t \geq 0$

$$(f_t \otimes g_p)(t) = \inf_{0 \leq s < T_f} (f_t(s) + g_p(t - s))$$

Then, for $t \geq T_f + T_g$, $0 \leq s < T_f \rightarrow t - s \geq T_g$. Thus,

$$\begin{aligned} (f_t \otimes g_p)(t + d_g) &= \inf_{0 \leq s < T_f} (f_t(s) + g_p(t + d_g - s)) \\ &= \inf_{0 \leq s < T_f} (f_t(s) + g_p(t - s)) + c_g \\ &= (f_t \otimes g_p)(t) + c_g \end{aligned}$$

□

Finally, for the fourth and last term:

Theorem 7 (Convolution of periodic parts). $f_p \otimes g_p$ is pseudo-periodic from $T = T_f + T_g + d$, with length $d = \text{lcm}(d_f, d_g)$ and increment $c = d \cdot \min(\rho_f, \rho_g)$.

To compute the convolution, we need slices

- $f_p \in [T_f, T_f + 2d[$
- $g_p \in [T_g, T_g + 2d[$

The convolution is then computed over interval

$$[T_f + T_g, T_f + T_g + 2d[$$

Proof. Since f_p and g_p are defined as above, we can write:

$$\begin{aligned} (f_p \otimes g_p)(t) &= \inf_{0 \leq s \leq t} f_p(s) + g_p(t - s) \\ &= \inf_{T_f \leq s \leq t - T_g} f_p(s) + g_p(t - s) \\ &= \inf_{a \geq T_f, b \geq T_g, a + b = t} f_p(a) + g_p(b) \end{aligned}$$

Then, for $t \geq T_f + T_g + d$

$$\begin{aligned} (f_p \otimes g_p)(t + d) &= \inf_{a \geq T_f, b \geq T_g, a + b = t + d} f_p(a) + g_p(b) \\ &= \min\left(\inf_{a' \geq T_f, b' \geq T_g, a' + b' = t} f_p(a' + d) + g_p(b'), \right. \\ &\quad \left. \inf_{a' \geq T_f, b' \geq T_g, a' + b' = t} f_p(a') + g_p(b' + d)\right) \end{aligned}$$

Here, we split the infimum in the min of two expressions, where term d appears as an argument of f_p and g_p , respectively, so that later on we can leverage the pseudo-periodic property for either function. To a closer inspection, the first case is equivalent to limiting $a \in [T_f + d, t + d]$, $b \in [T_g, t]$, whereas the second term is equivalent to limiting $a \in [T_f, t]$, $b \in [T_g + d, t + d]$.

One can verify that this covers all the possible cases, thus the split is valid.

Furthermore, having $a \in [T_f + d, t + d]$ (in the first term) and $b \in [T_g + d, t + d]$ (in the second term) means that we are, for all values in the range, to the right of the first pseudo-period of size d for that function, and we can thus apply the pseudo-periodic property.

Since $d = \text{lcm}(d_f, d_g)$, it is a multiple of both d_f and d_g . We can compute $k_f = d/d_f$ and $k_g = d/d_g$, $k_f, k_g \in \mathbb{N}$.

Thus, the two terms can be written as:

$$\begin{aligned}
 (f_p \otimes g_p)(t + d) &= \\
 &= \min \left(\inf_{a \geq T_f, b \geq T_g, a+b=t} f_p(a) + g_p(b) + k_f \cdot c_f, \inf_{a \geq T_f, b \geq T_g, a+b=t} f_p(a) + g_p(b) + k_g \cdot c_g \right) \\
 &= \inf_{a \geq T_f, b \geq T_g, a+b=t} f_p(a) + g_p(b) + \min(k_f \cdot c_f, k_g \cdot c_g) \\
 &= (f_p \otimes g_p)(t) + \min(k_f \cdot c_f, k_g \cdot c_g) \\
 &= (f_p \otimes g_p)(t) + d \cdot \min(\rho_f, \rho_g)
 \end{aligned}$$

□

Minimum of the four terms

It is important to observe that – in the general case – we cannot compute *a priori* the value of T for the minimum of the four terms. This is relevant, since it is what forces one to implement convolution by decomposing it into the four partial convolutions – plus a minimum –described above.

In fact we have that:

- The first term has no pseudo-periodic behavior, so it does not affect this discussion;
- The second term (call it C_2) has $\rho_2 = \rho_g$;
- The third term (call it C_3) has $\rho_3 = \rho_f$;
- The fourth term (call it C_4) has $\rho_4 = \min(\rho_f, \rho_g)$.

Consider the case of $\rho_f > \rho_g$. We can compute $\min(C_2, C_4)$ to have $T = \max(T_2, T_4) = T_f + T_g + d$ and $d = \text{lcm}(d_2, d_4) = \text{lcm}(d_f, d_g)$. However, for $\min(C_3, \min(C_2, C_4))$ we have $T = \max(T_f + T_g + d, \bar{t})$, where \bar{t} is the bound for the intersection of the two curves, which we cannot determine *a priori* as we do not know the shape of the partial convolutions.

This is not true if $\rho_f = \rho_g$, however, in which case we can determine that the minimum of the partial convolution has $T = T_f + T_g + d$. In fact, under this hypothesis, we can compute the entire convolution in a single by-sequence convolution. We thus obtain the following:

Theorem 8 (Convolution of curves with the same slope). *If $\rho_f = \rho_g$ ($= \rho$), then $f \otimes g$ has*

- $T = T_f + T_g + d$
- $d = \text{lcm}(d_f, d_g)$
- $c = \rho \cdot d$

The entire convolution can be computed using sequences S_f^D, S_g^D with $D = [0, T_f + T_g + 2d[$, and then computing the convolution of these sequences $S_{f \otimes g}^D$ over the same interval.

Proof. See the above discussion.

□